The GEWEX Water Vapor Assessment archive of water vapour products from satellite observations and reanalyses

Marc Schröder[1], Maarit Lockhoff[1], Frank Fell[2], John Forsythe[3], Tim Trent[4,5], Ralf Bennartz[6,7], Eva Borbas[7], Michael G. Bosilovich[8], Elisa Castelli[9], Hans Hersbach[10], Misako Kachi[11], Shinya Kobayashi[12], E. Robert Kursinski[13], Diego Loyola[14], Carl Mears[15], Rene Preusker[16], William B. Rossow[17], Suranjana Saha[18]

[1]Satellite-Based Climate Monitoring, Deutscher Wetterdienst, 63067 Offenbach, Germany
[2]Informus GmbH, Berlin, Germany
[3]Cooperative Institute for Research in the Atmosphere, Colorado State University, Fort Collins CO, USA
[4]Earth Observation Science, Department of Physics and Astronomy, University of Leicester, University Road, Leicester, LE1 7RH, UK
[5]National Centre for Earth Observation, Department of Physics and Astronomy, University of Leicester, University Road, Leicester, LE1 7RH, UK
[6]Earth & Environmental Sciences Department, Vanderbilt University, Nashville TN, USA
[7]Cooperative Institute for Meteorological Satellite Studies, Space Science and Engineering Center, University of Wisconsin - Madison, USA
[8]Global Modelling and Assimilation Office, Goddard Space Flight Center, National Aeronautics and Space Administration, Greenbelt MD, USA
[9]Institute of Atmospheric Sciences and Climate, National Research Council of Italy, Bologna, Italy
[10]European Centre for Medium-Range Weather Forecasts, Reading, UK
[11]Earth Observation Research Center, Japan Aerospace Exploration Agency, Tsukuba, Japan
[12]Japan Meteorological Agency, Tokyo, Japan
[13]Space Sciences and Engineering, Boulder CO, USA
[14]Remote Sensing Technology Institute, German Aerospace Center, Oberpfaffenhofen, Germany
[15]Remote Sensing Systems, Santa Rosa CA, USA
[16]Institute for Space Sciences, Free University of Berlin, Berlin, Germany
[17]CUNY Remote Sensing Science and Technology Institute, City College of New York, New York NY, USA
[18]Environmental Modeling Center, NCEP/NWS/NOAA, NCWCP, College Park MD, USA

Correspondence to: Marc Schröder (marc.schroeder@dwd.de)

Abstract. The Global Energy and Water cycle Exchanges (GEWEX) Data and Assessments Panel (GDAP) initiated the GEWEX Water Vapor Assessment (G-VAP), which has the main objectives to quantify the current state of art in water vapour products being constructed for climate applications and to support the selection process of suitable water vapour products by GDAP for its production of globally consistent water and energy cycle products. During the construction of the G-VAP data archive, freely available and mature satellite and reanalysis data records with a minimum temporal coverage of 10 years were considered. The archive contains total column water vapour (TCWV) as well as specific humidity and temperature at four pressure levels (1000, 700, 500, 300 hPa) from 22 different data records. All data records were remapped to a regular longitude/latitude grid of 2°x2°. The archive consists of four different folders: 22 TCWV data records covering the period 2003-2008, 11 TCWV data records covering the period 1988-2008, as well as seven specific humidity and seven

temperature data records covering the period 1988-2009. The G-VAP data archive is referenced under the following digital object identifier (doi): http://dx.doi.org/10.5676/EUM_SAF_CM/GVAP/V001. Within G-VAP, the characterisation of water vapour products is, among other ways, achieved through intercomparisons of the considered data records, as a whole and grouped into three classes of predominant retrieval condition: clear-sky, cloudy-sky and all-sky. Associated results are

5 shown using the 22 TCWV data records. The standard deviations among the 22 TCWV data records have been analysed and exhibit distinct maxima over central Africa and the tropical warm pool (in absolute terms) as well as over the poles and mountain regions (in relative terms). The variability in TCWV within each class can be large and prohibits conclusions on systematic differences in TCWV between the classes.

1 Introduction

10 Water vapour is the most important natural greenhouse gas and the dominant source of infrared opacity in the clear-sky atmosphere (Trenberth et al., 2007). In addition, fast acting water vapour feedbacks constitute a strong amplification mechanism for anthropogenic climate change (e.g., Held and Soden, 2000), thus, making water vapour also a key parameter for the energy budget of the Earth and consequently also for climate change analysis. Furthermore, the interactions of water vapour with other components of the climate system such as clouds and precipitation are still not fully understood.

15 Analysing recent decades of global water vapour distribution and variability is expected to help extend our understanding of how the climate system responds to increasing greenhouse gas concentrations. Due to global coverage and observing periods approaching 40 years satellite-based water vapour data records are adequate sources of information to address the above mentioned challenges and to analyse the Earth's climate.

To date, a large variety of satellite based water vapour data records is available. Information on such records is provided by

20 the ECV (see Table A1 in the Appendix for a list of abbreviations) inventory (http://climatemonitoring.info/ecvinventory), the Climate Data Guide (https://climatedataguide.ucar.edu/), and the Advancing Reanalysis web portal at http://reanalyses.org/. Without proper background information and understanding of the limitations of available data records, these data may be utilised incorrectly or misinterpreted. The need for quality assessments of ECV Climate Data Records is part of the GCOS guidelines for the generation of data products. Assessments in general provide an overview of available

25 data records and enable users to judge the quality and fitness for purpose of Climate Data Records by informing them about the strengths and weaknesses of existing and readily available records. With this in mind, GDAP has initiated G-VAP whose major purpose is to quantify the current state of the art in water vapour products being constructed for climate applications and to support the selection process of suitable water vapour products by GDAP for its production of global water and energy cycle products. Within G-VAP, efforts started with an inventory of freely available water vapour data records.

30 Overview tables for satellite, reanalyses, in-situ and ground-based data records are provided at http://gewex-vap.org/?page_id=13. Satellite and reanalyses products with a minimum length of 10 years are basic elements of the G-VAP data archive and form the basis for subsequent analysis in the characterisation effort of such data records. An archive of a

large variety of cloud data records has also been released by the GEWEX Cloud Assessment (Stubenrauch et al., 2012) which is available at http://climserv.ipsl.polytechnique.fr/gewexca/index-2.html.

In Sect. 2, an overview of previous and currently available satellite sensors together with a brief outlook on upcoming missions relevant for the retrieval of water vapour is presented. The focus of Sect. 3 is a table of existing satellite and
5   reanalyses data records. The G-VAP data archive is introduced in Sect. 4 which is based on a subset of data records introduced in Sect. 3. Sect. 4 starts with a brief introduction of all data records included in the archive. Then, the processing of the data records and the archive structure are explained. The following section includes exemplary results from the intercomparison of the data records from the G-VAP data archive. Here, TCWV data records with temporal coverage from 2003 to 2008 are considered so that all data records of the archive are included. Conclusions are given in Sec. 7. In Appendix
10   A a list of abbreviations is provided.

2 Overview of available satellite sensors

In this section, background information on the wide variety of sensors that measure atmospheric water vapour is provided. Only sensors that have a greater than 10-year record and that cover (near) global scales, are discussed. These are the types of sensors used to create global climate data records of water vapour.

15   Generally water vapour sensors are deployed on low-Earth orbiting and geostationary satellites. Sensors that provide (near) global coverage typically operate on polar orbiting platforms in a sun-synchronous orbit. Such sensors provide global coverage with one day-time (at a particular local time) and one night-time overpass (12 hours later). Instruments classified as sounders carry several channels distributed about a water vapour absorption line to retrieve the vertical profile of water vapour. Instruments classified as imagers might also have channels clustered about an absorption line, but the primary
20   purpose of an imager is to sense the surface or cloud tops. Imagers are generally restricted to only retrieving TCWV.

The term "profile" usually implies the water vapour amount (mixing ratio) on a given set of pressure levels, such as those measured by a radiosonde. Satellite sounding instruments respond to radiation from a great depth of the atmosphere as depicted by the instrument weighting function, so the retrieval of atmospheric layers is the natural unit here. These layers might be interpolated to pressure levels to compare with, for instance, a radiosonde or a model, but users should remain
25   aware of the broad vertical layer over which satellite sounders nominally average.

This section approaches the overview of sensors from the standpoint of where and what they sample, and the pros and cons of each sensor from a user perspective. Chronological listings are readily available, for instance in Kämpfer (2012; Figure 9.1). A recent overview on sensors is also provided by Wulfmeyer et al. (2015). The information provided here is a snapshot in 2017, but radiance records and sensor intercalibration continue to progress, and algorithm improvements can expand the
30   yield and performance of remote retrievals of water vapour. This list is not meant to be exhaustive, but serves to orient the climate user to the major sensors supporting the water vapour climate data record and their pros and cons. Sensors based on limb sounding techniques that focus on the upper atmosphere are not considered in this report. Information on these

techniques and associated data records can found at the SPARC Water Vapour Assessment 2 web portal: http://www.sparc-climate.org/activities/water-vapour/.

There are a wide variety of water vapour sensors currently operating, and for climate research the sensors change and vary through time. Understanding which sensors were operating at any given time period is a major endeavour. The World

5 Meteorological Organization has created an online tool which makes this task much more feasible. The Observing Systems Capability Analysis and Review Tool is maintained at http://www.wmo-sat.info/oscar/.

In Table 1, a summary of the main sensors used for global water vapour climate data records is presented.

2.1 Passive microwave sensors

Passive microwave sensors are typically classified as imagers and sounders. Some instrument names indicate the principal

10 mission of the sensor, e.g. SSM/I, its successor SSMIS or AMSU. Regardless of the classification of the sensor, both imagers and sounders allow water vapour retrievals in clear and cloudy skies, but not in the presence of strong scattering by hydrometeors like during heavy precipitation events.

The passive microwave radiance record, both from imagers and sounders with either a conical or cross-track scan pattern and a few non-scanning, nadir-looking instruments has exhibited good overlap and continuity since the late 1980's, early 1990's

15 to the present. The primary spectral bands represented in the climate record are radiances at 19, 22, 37, 50-60, 85-90, and 183 GHz. This record will continue with future sensors such as the Microwave Imager and Microwave Sounder instruments on EPS-SG, which is planned to measure until ~2040. Intercalibration efforts among the sensors (e.g. Sapiano et al., 2013 and Fennig et al., 2015) yield fundamental climate data records that can be used to remove time-dependent changes in the radiance record. Intercalibration efforts for the 183 GHz radiance record continue to move forward (e.g. John et al., 2012 and

20 Chung et al., 2013).

Conical scanning microwave imagers are typically configured at an Earth incidence angle of about 53 degrees. They have the advantage of constant spatial resolution across the scan, and constant sensitivity to the atmosphere via the same geometric path length. Microwave surface emissivity over land and ocean is a function of incidence angle, so, in principle conical scanners eliminate this variable from atmospheric retrievals. Cross-track scanners have changing spatial resolution which is

25 highest at near-nadir views and grows into larger fields-of-view at the outer edge of the scan. They have a minimal atmospheric path length at nadir.

1987 saw the launch of the first SSM/I instrument, a sensor that, while having no official climate mission, has had a profound impact on global water vapour records. The water vapour absorption line at 22 GHz is a key component of these TCWV retrievals, other window channels compensating for cloud and surface roughness effects.

30 TCWV from passive microwave imagers has historically only been retrieved over the ice-free oceans, and it is commonly although incorrectly stated that passive microwave retrievals work over ocean only. This is due to complex and variable land surface emissivity that changes on short timescales due to surface wetness, vegetation state, and soil properties. The barrier to passive microwave retrievals over land is beginning to fall, at least for operational weather users, as evidenced for

instance by the NOAA Microwave Integrated Retrieval System (Boukabara et al., 2011; Forsythe et al., 2015). Du et al. (2015) demonstrate an AMSR2 algorithm to retrieve TCWV over land. AMSR2 on board the Global Change Observation Mission – Water is a successor of AMSR-E on board Aqua, and has the highest spatial resolution among passive microwave imagers on polar orbiting platforms. Land retrievals require further investigation for climate research. For the water vapour climate record the passive microwave TCWV record has not yet been demonstrated over land, but there is some possibility of this advance in the coming years.

2.2 Infrared sensors

Infrared sounding sensors constitute the longest type of satellite record for water vapour profiling. A key distinction between infrared sensors for water vapour retrievals is between radiometers (e.g., HIRS, ATSR) and spectrometers (e.g., AIRS, IASI, CrIS). The broadband observations of radiometers constitute a longer time series (versions of the HIRS instrument extend back to the early 1980's), while the hyperspectral observations of spectrometers enable retrievals with more vertical information and improved uncertainty. The hyperspectral climate record begins with AIRS in 2002, and is augmented by the IASI instrument onboard the Metop-A and –B spacecrafts launched in 2006 and 2012 respectively. The CrIS instrument onboard the Suomi- National Polar-orbiting Partnership spacecraft launched in 2011 and on successor JPSS spacecraft continue the hyperspectral sounding record. A third IASI instrument is due for launch end of 2018 onboard Metop-C, which will extend the IASI mission and the associated sounding products from 2006 to beyond 2023. IASI's successor, IASI-NG, will be onboard the EPS-SG satellite, providing hyperspectral observations until ~2040. Beginning with Metop-C and due to the availability of IASI, HIRS will not be continued. In February 2016 Sentinel 3 was launched which carries the SLSTR instrument, a successor of the ATSR instrument series.

Infrared-only retrievals of TCWV and water vapour profile are retrieved under clear-sky or mostly clear-sky conditions only. The combination with passive microwave sounders improves the range of sky conditions in which retrievals are possible (e.g. Li et al., 2000; Kahn et al., 2014). The intercalibration of the HIRS record is still continuing (e.g. Shi et al., 2008). There are intersensor differences in the spectral placement of the 20 channels on HIRS and most impactful is the switch of channel 10 from 8.6 µm to 12.5 µm on the HIRS 3 and 4 sensors beginning with NOAA-15 in 1998.

While land surface emissivity is much more uniform and less time-varying in the infrared than at microwave wavelengths, infrared land surface emissivity does vary (Seemann et al., 2008) and can be problematic for infrared retrievals, especially over desert surfaces.

2.3 Ultraviolet/Visible/Near-Infrared imagers

A retrieval using two channels at 0.885 µm (window) and 0.9 µm (water vapour absorption) has been demonstrated from the MERIS instrument (Lindstrot et al., 2014). The retrieval is limited to the daylight portion of the swath, as differential solar reflectance is the signal for this retrieval. These types of retrievals have the benefit of high spatial resolution (~ 1 km). The MERIS instrument was launched in 2002, while MODIS onboard the Terra spacecraft begins in 1999, and is complemented

by the MODIS onboard the Aqua spacecraft which was launched in 2002. In February 2016 Sentinel 3 was launched which carries OLCI instrument on Sentinel 3, a successor of the MERIS instrument. MERIS stopped operation in April 2012 while the TCWV time series can be extended with data from MODIS and OLCI. Retrievals from MERIS, MODIS and OLCI complement passive microwave TCWV retrievals because they perform best over land and have reduced quality over

5   oceans.

UV/VIS/NIR spectrometers such as GOME, SCIAMACHY, and GOME-2 yield retrievals of total column water vapour over land and ocean surfaces under daylight and clear-sky conditions (Grossi et al., 2015). The spatial resolution is between 320 km x 40 km for GOME, 60 km x 30 km for SCIAMACHY, and 80 km x 40 km for GOME-2, with cloud handling being a major challenge.

10   A recent development in remote sensing of water vapour is the retrieval of TCWV from the NASA Orbiting Carbon Observatory (OCO-2) spacecraft (Nelson et al. 2016). This retrieval uses near-infrared reflected sunlight with the high quality OCO-2 grating spectrometer.

Future European missions such as Sentinel-5 precursor, EPS-SG, and Sentinel-5 will carry similar UV/VIS/NIR spectrometers with improved spatial resolution (<10 km) which will further extend the total column water vapour records

15   from UV/VIS/NIR spectrometers.

2.4 GPS Radio Occultation

GPS-RO measurements profile atmospheric refractivity with globally-distributed, all-weather sampling from which tropospheric water vapour is derived. GPS-RO missions began with the prototype GPS-MET mission from April 1995 – Feb. 1997. The CHAMP mission provided about 250 occultations per day from 2001 to 2010. A significant increase in RO

20   sampling density to 2,000-2,500 occultation profiles per day began with the launch of the 6-satellite COSMIC mission in April 2006. The COSMIC orbits were spread in longitude to provide full sampling of the diurnal cycle. The GRAS GPS-RO instruments, flying onboard Metop-A and Metop-B since 2007 and 2012, respectively provide occultation swaths centered on 9:30 and 21:30 local time. The CHAMP occultation profiles only penetrate down into the upper to middle troposphere because the GPS receiver on CHAMP was limited to closed-loop tracking. The COSMIC and GRAS GPS-RO receivers use

25   an "open-loop" tracking capability that enable a far higher percentage of the occultation profiles to extend to within 1 km of the surface.

From the GPS-RO receiver phase measurements during each occultation, the bending of the signal path due to its passage through the atmosphere is determined. The bending angle profile is then inverted to a profile of index of refraction which is closely related to the dry gas and water vapour concentrations. The water vapour contribution is typically isolated using one

30   of two approaches. The first is a variational technique used in numerical weather prediction assimilation systems where estimates of the water vapour, temperature and pressure from the forecast and their associated error covariances are combined with the GPS occultation bending angle or refractivity profile and its error covariance to achieve a new, statistically optimal estimate (e.g. Healy and Eyre, 2010). The second approach, referred to as the "Direct" method, estimates

the dry part of the refractivity from the analysis temperature that is then subtracted from the GPS-measured total refractivity to obtain the wet part of the refractivity, which is then scaled to obtain the water vapour. Both methods rely on the analysis temperatures that are a combination of observations and the numerical weather prediction model. The advantage of the Direct method is that it does not rely on estimates of water vapour from models, forecasts or climatologies. Estimates of the

5   systematic and random uncertainties of water vapour derived from COSMIC observations via the Direct method are given in Kursinski and Gebhardt (2014).

GPS-RO has very high vertical resolution for a satellite system (100-200 m) and relatively coarse horizontal resolution of about 100 km (Kursinski et al., 1997, eqn. 13). The altitude range of GPS-RO individual profiles of water vapour extends from the surface to about the 240 K-temperature level in the troposphere.

10   GPS-RO's ability to routinely penetrate through clouds combined with its insensitivity to surface emissivity eliminates sampling biases that limit other satellite measurement systems. A caveat with present GPS-RO derived water vapour is that in warm conditions typically found in low latitudes in particular, GPS-RO water vapour profiles in the boundary layer can be biased low when a sharp water vapour concentration contrast exists between dry free tropospheric air and moist boundary layer air below, causing the so called super-refraction (e.g., Xie et al., 2006).

15   Xie et al (2006) developed an inversion method that accounts for super-refraction and produces unbiased water vapour profiles in the boundary layer. Because it has been difficult to determine when super-refraction is occurring in the COSMIC profiles, the Xie et al method has not yet been used much. To overcome this challenge, the new GPS-RO receivers on COSMIC 2 are designed to provide much higher signal-to-noise ratios to enable routine detection of super-refraction.

The COSMIC 2 mission is scheduled to launch 6 satellites in 2017 and possibly a second set sometime later. Successors of

20   GRAS will fly on EPS-SG with a sustained operation until ~2040.

2.5 Reanalyses

Reanalysis systems are typically based on advanced operational atmospheric general circulation models and include data assimilation schemes. The aata assimilation merges spatially and temporally discontinuous observations with model state fields to reinitialize atmospheric forecasts and produce spatially and temporally continuous state fields. The data assimilation

25   schemes differ among each other by the degree of complexity, by the assimilation strategy (i.e., assimilation of geophysical parameters versus assimilation of radiances) and by data input. All major reanalyses assimilate a large diversity of data from observing system like radiosondes, ground-based GPS and GPS-RO, diverse satellites, buoys and ships and more. Reanalyses are performed with a fixed model and data assimilation system, however data input to the reanalysis system changes over the years. Reanalysis products are generated retrospectively, and several reanalysis centres provide near real

30   time services. The major purpose is to provide a product which allows the analysis of the weather and climate and how it changes over time. Reanalyses provide global coverage and cover the full troposphere and stratosphere. An advantage is the large diversity of gap-free geophysical parameters. Reanalyses rely on atmospheric numerical models which carry their own systematic biases and which is a disadvantage. Diversity in the assimilated observations in each system, the quality control

and the varying number of observations in space and time can affect the reanalysis quality. More information can be found in the references given in Table 2 as well as at http://www.reanalyses.org and at http://s-rip.ees.hokudai.ac.jp/, the webpage of the SPARC Reanalysis Intercomparison Project.

3 Overview of data records

5   Using observations from satellites and data from reanalyses, as introduced in the previous section, a large variety of (global) long-term water vapour data records have been developed over the last decades and are freely available. An overview of such data records from satellite and reanalyses is provided in Table 2. The table is based on the information available on the G-VAP website at http://gewex-vap.org/?page_id=13, where also tables for operational satellite as well as in-situ and ground-based products are available. The first column of Table 2 gives the sensor while the second one contains the data

10   record name. Subsequently this name is used. If not available or unique the data record is named after the utilised sensor and the owner. Besides the covered parameter and key references, the main technical specifications are provided which might allow a first order decision on the fitness-for-purpose of a particular data record. Other information sources on water vapour data include the ECV inventory (http://climatemonitoring.info/ecvinventory), the Climate Data Guide (https://climatedataguide.ucar.edu/), and the http://reanalyses.org/ website.

15   Note that in this section a general overview of available data records is provided and that not all data records mentioned in Table 2 are part of the G-VAP data archive. A few more details regarding retrieval scheme and other details are provided in short paragraphs per data record of the G-VAP data archive in Sect. 4.1.

4 G-VAP data archive

In this section the G-VAP data archive is introduced. At first it is explained why the G-VAP data archive consists of a subset

20   of the data records mentioned in Table 2. GDAP has initiated G-VAP, among others with the purpose of G-VAP to support the selection process of suitable water vapour products by GDAP for its production of globally consistent water and energy cycle products. The usage of the products within GDAP activities essentially implied to study long-term data records. G-VAP considered all data records "long-term" that are longer than ten years. Thus, the assessment considered data records that may not be used as input for GEWEX water and energy cycle data records but which are important to establish a deep

25   understanding of atmospheric water vapour observations. This considerably increased the number of data records that can be analysed. It is further requested that the data is freely available. However, a few data records of the G-VAP data archive have been provided by the data record's principle investigator. After August 2016 the filling and updating of the G-VAP data archive ended in order to allow a timely analysis of the data and provision of results to GDAP. Thus data records that exceed a temporal coverage of more than 10 years by the end of 2015 are considered. The data records that comprise the G-VAP

30   data archive are marked with an asterisk in Table 2.

It follows a short description of the individual data records, of the post-processing and of the archive structure.

4.1 Introduction to individual data records

Below a short introduction to each data record of the G-VAP data archive is given.

AIRWAVE

The AIRWAVE retrieval scheme exploits the dual view capabilities of the ATSR instrument series by using the two thermal infrared channels, centred at 10.8 and 12 µm. It works above the cloud-free ocean by combining advanced radiative transfer models and a sea surface spectral emissivity database. The simultaneous use of ATSR's forward and nadir measurements minimises the impact of the limited knowledge about the sea surface temperature and the atmospheric radiation on the quality of the retrieved TCWV. Exploiting only the thermal infrared channels of the instrument, the algorithm enables the estimation of TCWV for both day and night observations and the full exploitation of the ATSR instrument series, spanning from 1991 to 2012 (see Casadio et al., 2016 and Castelli et al., 2015 for details). The AIRWAVE processor is integrated in the ESA Grid Processing on Demand environment for the bulk processing of the three ATSR missions (1991-2012). The product is available in Level 2 (1×1 km^2 and $0.25° \times 0.25°$). The AIRWAVE version 1 data record was provided as monthly means at a spatial resolution of $1° \times 1°$ via ftp in June 2015.

AMSR-E JAXA

The AMSR-E standard TCWV algorithm uses AMSR-E brightness temperatures at 18.7, 23.8, 36.5 GHz channels for V/H polarization, and sea surface temperature, sea surface wind speed, temperature at 850 hPa given by Japan Meteorological Agency 6-hourly global analysis data as ancillary data (see Takeuchi, 2002 and Takeuchi et al., 2004 for details). The algorithm is applicable to open ocean regions only and its dynamic range is 0-70 kg/m^2. The product is available in Level 2 (swath data with about 10 km sampling intervals) and Level 3 (daily, monthly, $0.25° \times 0.25°$ grid for ascending and descending orbits) from June 2002 to October 2011. The latest AMSR-E version 7 product has been released to public in July 2011. Its accuracy is 2.9 kg/m^2 in RMSD compared with global radiosonde data from 2002 to 2009, and 1.9 kg/m^2 compared with GPS TCWV from 2004 to 2008 around Japan. The reprocessing of the AMSR-E TCWV product is underway along with other AMSR-E geophysical parameter products by applying the latest AMSR2 algorithm (see Kazumori et al., 2012 and Kazumori, 2013 for TCWV) in order to produce consistent AMSR-E/AMSR2 products covering more than 15 years. The AMSR-E JAXA version 2 was downloaded as monthly means from https://gcom-w1.jaxa.jp/auth.html in February 2015.

AMSR-E REMSS

The REMSS AMSR-E vapour algorithm is part of a multi-parameter retrieval scheme that simultaneously retrieves TCWV, surface wind speed, sea surface temperature, and cloud liquid water content and rain rate for ocean scenes. The basic

algorithm is described in Wentz (1997), with updated models of the microwave absorption, emission, and scattering by the atmosphere and ocean surface (Meissner and Wentz, 2012; Wentz and Meissner, 2017). The algorithm most strongly depends on the 23.8 GHz, on the upper wing of the water vapour line at 23.235 GHz, with the other AMSR-E channels providing information about surface roughness and atmospheric scattering and absorption from liquid water. The data are

5 available as twice-per-day near-global gridded maps with 0.25°×0.25° resolutions from http://www.remss.com/missions/amsr.html. The TCWV values have been validated via comparison with similar measurements from TMI (Wentz, 2015) and with TCWV measurements made by ground based GNSS sensors located on small islands (Mears et al., 2015). Monthly means of AMSR-E REMSS V7 have been downloaded in March 2015.

10 ATOVS

The CM SAF ATOVS data record offers 13 years (1999 - 2011) of satellite-derived global water vapour and temperature products. Different parameters are generated simultaneously: total column water vapour [kg/m^2], mean temperature [K] and vertically integrated water vapour [kg/m^2] in 5 layers, as well as specific humidity [g/kg] and temperature [K] at 6 levels. Also available are the number of valid observations and an uncertainty estimate. The data record was derived from ATOVS

15 on-board NOAA-15 to -19 and Metop-A. ATOVS is composed of three instruments: HIRS, AMSU-B/MHS and AMSU-A. After application of a kriging routine, the products are available as daily and monthly means on a cylindrical equal area projection at a resolution of 90 km × 90 km. Grid information is given for centre position. Layers are [hPa]: 200-300, 300-500, 500-700, 700-850, and 850-surface. Levels are [hPa]: 200, 300, 500, 700, 850, and 1000. Further details on the retrieval and on validation results can be found in Courcoux and Schröder (2015). Also, the validation report, algorithm theoretical

20 basis document and product user manual can be downloaded from http://www.cmsaf.eu/docs. The data record is doi-referenced (10.5676/EUM_SAF_CM/WVT_ATOVS/V001) and accessible via http://wui.cmsaf.eu. Here, ATOVS version 1 was utilised, which was downloaded in April 2013.

CFSR

25 The NCEP CFSR was designed and executed as a global, high-resolution coupled atmosphere–ocean–land surface–sea ice system to provide an estimate of the state of these coupled domains over the period from 1979 to the present, currently being run as an operational, real-time product. The CFSR include 1) coupling of the atmosphere and ocean during the generation of the 6-hour guess field, 2) an interactive sea ice model, and 3) assimilation of satellite radiances by the Gridpoint Statistical Interpolation scheme over the entire period. The CFSR global atmosphere resolution is ~38 km (T382) with 64 levels

30 extending from the surface to 0.26 hPa from 1979-2009, and is ~25 km (T574) after that. The CFSR atmospheric model has observed variations in CO_2 over the 1979–present period, together with changes in aerosols and other trace gases and solar variations. Most available in-situ and satellite observations were included in the CFSR. Satellite observations were used in radiance form, rather than retrieved values, and were bias corrected with "spin up" runs at full resolution, taking into account variable CO_2 concentrations. CFSR output products are available at an hourly time resolution and a horizontal resolution of

0.5° latitude × 0.5° longitude. More details are given in Saha et al. (2010). The CFSR data is distributed by the National Center for Environmental Information and National Center for Atmospheric Research. The temperature as well as TCWV and specific humidity profile data records have been accessed via https://rda.ucar.edu/datasets/ds093.2/ in March 2016 and June 2013, respectively.

EMiR

The MWR instrument flown onboard the European Remote Sensing satellites 1 and 2 as well as onboard the Environmental Satellite has provided a time series of global microwave observations over a period of nearly 21 years between 1991 and 2012. The EMiR data record builds on the MWR time series by applying a one-dimensional variational approach to provide

10 information on TCWV and wet tropospheric correction in clear and cloudy-sky conditions. Significant efforts were invested to ensure a good intercalibration of the three MWR instruments. Details on the retrieval and results from validation are given in Bennartz et al. (2017). The EMiR data record covers the entire global ice-free ocean from 11/1992 to 03/2012. It is available for individual orbits (Level-2) at a spatial resolution of typically 20 km as well in a gridded form (Level-3) for monthly mean values at 2°×2° and 3°×3° spatial resolution. The EMiR data record and supporting information can be

15 obtained free of charge from http://dx.doi.org/10.5676/DWD_EMIR/V001. The EMiR data record (version 1) was downloaded in May 2016.

ERA-Interim

The ECMWF ERA-Interim reanalysis (Dee et al., 2011) provides globally complete atmospheric products from 1979

20 onwards at a mixed 3-hourly/6-hourly output frequency and is continued with updates available at about 3 months behind real time. Its atmospheric general circulation model and 4D-Var assimilation system are based on the version of the ECMWF integrated forecast system that was used in the ECMWF operational system between 12 December 2006 and 5 June 2007 (Cy31r2). It is conducted at reduced resolution, though, of about 79 km in the horizontal (T255 in spectral space) and 60 levels in the vertical from the surface to 0.1 hPa. ERA-Interim is the predecessor of the ERA5 reanalysis, which is currently

25 in production (Hersbach and Dee, 2016). ERA-Interim incorporates an improved representation of the hydrological cycle, 4D-Var, the implementation of variational bias control for satellite radiances and the assimilation of TCWV satellite retrievals using the 1D+4D-Var approach (Bauer et al., 2006a, b). Over the global oceans boundary conditions are provided by prescribed estimates for SST and sea-ice cover. ERA-Interim exploits in situ measurements of surface pressure, 2m temperature, 2m relative humidity from land stations, ships and drifting buoys and near-surface wind from these latter two,

30 upper-air temperatures, wind, and specific humidity from radiosondes, pilot balloons, aircraft, and wind profilers. The largest amount of data comes from polar-orbiting and geostationary satellite observations, which are mostly assimilated as brightness temperature using suitable observation operators. In addition, satellite-derived atmospheric motion vector winds, information on surface wind from scatterometers, ozone retrievals, measurements from GPS radio occultation and ocean wave height from altimeters are ingested. Between 1992 and 2006 there is an artificial reduction in precipitation of about 0.1

mm/day over the global oceans, which can be traced back to a problem in the linearised moist physics in the 1D-Var observation operator in the above-mentioned 1D+4D-Var scheme (Geer et al., 2008). Monthly means of temperature as well as TCWV and specific humidity with a spatial resolution of 1°x1° were downloaded from http://apps.ecmwf.int/datasets/ in November 2012 and June 2016, respectively.

ERA-20C

The ECMWF twentieth century reanalysis ERA-20C (Poli et al., 2016) provides globally complete atmospheric estimates for the period 1900-2010 at a 3-hourly output frequency. Its atmospheric general circulation model and 4D-Var assimilation system are based on the version of the ECMWF integrated forecast system that was used in the ECMWF operational system

10 between 19 June 2012 and 25 June 2013 (Cy38r1). It was conducted though at a much reduced resolution of about 125 km in the horizontal (T159 in spectral space) and 91 levels in the vertical from the surface to about 80 km height (0.01 hPa). The radiative forcing includes the CMIP5-prescribed (Taylor et al., 2012) evolution of greenhouse gases, tropospheric and stratospheric (volcanic) aerosols and solar forcing, while the ocean surface is constrained by prescribed forcing from the HadISST2 SST and sea-ice product (see Hersbach et al., 2015 for details). ERA-20C only uses observations from surface

15 pressure, mean sea level pressure and marine wind, which were obtained from the International Surface Pressure Databank (Cram et al., 2015) version 3.2.6 and the International Comprehensive Ocean–Atmosphere Data Set (Woodruff et al., 2011) version 2.5.1. No humidity observations are assimilated and the analysis fields for water vapour are provided indirectly from the assimilated pressure and wind observations via the model equations in a physically meaningful way. Monthly means of TCWV, specific humidity and temperature with a spatial resolution of 1°x1° were downloaded from

20 http://apps.ecmwf.int/datasets/ in June 2016.

GOME/SCIAMACHY/GOME-2 GlobVapour

The GOME/SCIAMACHY/GOME-2 family of instruments are nadir-looking spectrometers operating in the UV/VIS/NIR wavelength region (SCIAMACHY has more extended capabilities as well, which are not considered here). The three

25 instruments operate on polar-orbiting satellites with a local crossing time of 10:30, 10:00 and 9:30, respectively. A spectral window around the H_2O absorption lines near 630 nm are used for the retrieval of TCWV both over ocean and over land surfaces under daylight and clear-sky conditions (Wagner et al., 2003).

The GlobVapour TCWV product from GOME/SCIAMACHY/GOME-2 is based on the GOME Data Processor 4.x algorithm (Grossi et al., 2015), as currently being used in the EUMETSAT Atmospheric Composition Monitoring SAF for

30 the generation of the operational TCWV products from GOME-2. The algorithm has two major steps: the Differential Optical Absorption Spectroscopy least-squares fitting for the trace gas slant column, followed by the computation of a suitable air mass factor to make the conversion to the vertical column density. The air mass factor algorithm used is optimised for generating self-consistent long-term climatological data, by minimising external inputs. Monthly time series of TCWV derived for each instrument are harmonised using GOME as reference. The product covers the period January 1996

until December 2008 and has a spatial resolution of 0.5°. The data record is accessible via http://globvapour.info/products.html#daftp and the version 1 was downloaded in June 2016.

HIRS UWisconsin

5   The HIRS UWisconsin moisture record retrieves TCWV as well as integrated high, mid, and low layer tropospheric humidity. TCWV and UTH are determined for clear-sky radiances measured by HIRS (at 20 km and later 10 km resolution) over land and ocean both day and night. The retrieval is a statistical regression (Seemann et al 2003 and 2008) developed from an atmospheric profile database (SeeBor, Borbas et al, 2005) that consists of geographically and seasonally distributed radiosonde, ozonesonde, and ECMWF reanalysis data. The AVHRR based Pathfinder Atmospheres - Extended cloud mask

10 is used to characterize HIRS sub-pixel cloud cover. The HIRS TCWV and integrated high layer tropospheric humidity products are binned into a global map of 0.5°x0.5°, for four time periods daily (night before and after midnight and day before and after noon), compiled into monthly amounts (for the operational months of each satellite), and inspected for trends over a 35-year period (1980-2015). The HIRS UWisconsin moisture package (version 2.5R2) was provided via ftp and downloaded in May 2016.

HOAPS

The HOAPS data record is a satellite based climatology of total column water vapour, near surface specific humidity, wind speed, precipitation, evaporation, latent heat flux and freshwater budget (evaporation minus precipitation) over the global ice-free oceans. All variables are derived from SSM/I passive microwave radiometers, except for SST, which is taken from

20 AVHRR measurements. The data record generation involves multi-satellite averages, inter-sensor calibration, and an efficient sea ice detection procedure. All HOAPS products have global coverage, i.e., within ±180° longitude and ±80° latitude and are only defined over the ice-free ocean surface. The products are available as monthly averages and 6-hourly composites on a regular latitude/longitude grid with a spatial resolution of 0.5°×0.5°. Grid information is given for cell centre position. More details on the water vapour retrieval and HOAPS in general can be found in Schlüssel and Emery

25 (1990) and Andersson et al. (2010). Also, the validation report, algorithm theoretical basis document, and product user manual can be downloaded from http://www.cmsaf.eu/docs. Starting with v3.1 the data is accessible via http://wui.cmsaf.eu. Here, HOAPS v3.2 was utilised, which was downloaded in March 2012.

JRA-55

30 JRA-55 is a global atmospheric climate dataset covering the period from 1958, when regular radiosonde observations began on a global basis, to the present. JRA-55 has been produced with the TL319 version of the Japan Meteorological Agency operational data assimilation system (as of December 2009), which features among others four-dimensional variational analysis (4D-Var) and variational bias correction for satellite radiances. The products are available as monthly, 6-hourly and 3-hourly (for surface parameters only) temporal resolutions on the TL319 quasi-regular Gaussian grid (approximately 55-km

resolution) as well as a regular latitude/longitude grid with a spatial resolution of 1.25°×1.25°. More details on general specifications and basic characteristics of JRA-55 can be found in Kobayashi et al. (2015). Also, JRA-55 product users' handbook can be downloaded from http://jra.kishou.go.jp/JRA-55/index_en.html. Monthly means of temperature as well as TCWV and specific humidity were downloaded from http://jra.kishou.go.jp/ in February 2015 and July 2016, respectively.

MERIS GlobVapour

The high spatial resolution TCWV data record was derived from ESA's 3rd reprocessing of the MERIS L1 archive. The TCWV retrieval is based on an optimal estimation approach and applied to swath-based, normalized radiances in MERIS bands at 865 nm, 885 nm, and 900 nm, while the cloud screening procedure utilises the full set of MERIS radiances between 400 and 900 nm. The product also includes information on uncertainties. Further details and results from validation are given in Lindstrot et al. (2012). The data record covers the period January 2003 – March 2012 and is available on a global grid at a spatial resolution of 0.05° over the coastal ocean, open ocean areas with occurring sun glint, and cloud free land surfaces. The data record (version 1) was provided via ftp in July 2015.

15 MERRA/MERRA-2

The original intent of the MERRA project was to improve upon the representation of the global water cycle in reanalyses (Rienecker et al., 2011). While there were some successes in MERRA, the changing observing system, particularly with sensors sensitive to water vapour, lead to spurious jumps in the global total column water column record. In attempting to improve on MERRA, MERRA-2 incorporates a mass conservation constraint on the dry mass and water vapour assimilation that results in the global water vapour analysis increment to be negligibly small, which has the result of a global evaporation and precipitation balance (Takacs et al., 2016; Gelaro et al., 2017). For total column water, this has led to a global time series that is much more stable than that of MERRA (Bosilovich et al., 2017). While the global water analysis increments are essentially zero, they can have a value at any given point or region, and the influence of the changing water vapour observations can also be apparent. In addition, over land surfaces, MERRA-2 uses observation corrected precipitation as the surface source of water, providing another observation constraint in the global water cycle (Reichle et al., 2017). Monthly means of temperature as well as TCWV and of specific humidity (MERRA) with a spatial resolution of 0.5°x0.66° were downloaded from https://goldsmr2.gesdisc.eosdis.nasa.gov/ in November 2012 and March 2013, respectively. MERRA-2 has a spatial resolution of 0.5°x0.625° and was downloaded from https://goldsmr5.gesdisc.eosdis.nasa.gov/ in April 2016.

30 MODIS AQUA

The MODIS TCWV data record was obtained from the Collection 5 MODIS Near-IR Products (called MOD05). The near-IR TCWV is derived from the attenuation by water vapour of near-IR solar radiation. Techniques (Gao and Kaufman, 2003) employing ratios of water-vapour-absorbing channels 17, 18, and 19 with the atmospheric window channels 2 and 5 are used. The ratios remove partially the effects of variation of surface reflectance with wavelength and result in atmospheric

water-vapour transmittances. The solar retrieval algorithm relies on observations of water-vapour attenuation of reflected solar radiation in the near-infrared MODIS channels so that the product is produced only over areas where there is a reflective surface in the near IR, during the daytime, over clear land areas of the globe and above clouds over both land and ocean. Over clear ocean areas, water-vapour estimates are provided over the extended glint area. The Level 2 data are

5 generated at the 1 km spatial resolution of the MODIS instrument. There are three MODIS Level 3 gridded atmosphere products: daily, 8-day, and monthly, where the Level 2 atmosphere products are aggregated to a 1° x 1° equal-angle global grid (called MOD08, Platnick et al., 2015). The MODIS MOD08 monthly mean TCWV data record was downloaded from https://ladsweb.modaps.eosdis.nasa.gov/search/order/2/MYD08_M3--6 in May 2015.

10 nnHIRS

The nnHIRS global atmospheric temperature-humidity profile data product is one of the products produced by the International Satellite Cloud Climatology Project and is based on new retrievals from re-calibrated HIRS measurements (Shi et al., 2016) with temporal (and some spatial) interpolations to provide global coverage every 3 hr over the period 1980 – 2015. The new retrievals differ from previous analyses of satellite HIRS measurements in four ways: (1) a cloud detection

15 algorithm is applied to each individual field of view (pixel) and all clear pixels are processed, (2) the retrieval procedure accounts for variations of CO_2 abundance over the record, (3) the retrieval procedure accounts explicitly for variations of surface topography and (4) the retrieval obtains values for near-surface air and skin temperatures separately. Because of cloud cover, the typical coverage of the globe on a given day is about 30% but only about 10-15% at a given time of day. This product provides global coverage every 3 hr from the new retrieval results by employing time-interpolation procedures,

20 including a specific statistical model of the diurnal variations of temperature in the lower troposphere over land. The humidity profile is extended into the stratosphere by combining the HIRS-based results with those from other satellite measurements of humidity (Davis and Rosenlof, 2016). The near-surface humidity over oceans is adjusted based on a matched analysis of satellite microwave observations to produce the SeaFlux products (Clayson et al., 2012). The near-surface temperatures over land are adjusted based on the global collection of surface weather observations (Smith et al.,

25 2011). Comparison of the resulting temperature-humidity profiles against space-time-matched radiosondes (over land, ARSA), AIRS profiles (V6 L2, Chahine et al., 2006) and ERA-Interim (Dee et al., 2011) profiles globally show RMSD of temperature generally less than 2 K, but 3 K near the land surface, and of specific humidity less than 20% relative, but 30% near the land surface (Rossow and Pearl, 2017). Monthly means of TCWV and specific humidity from the nnHIRS data record were provided via ftp in October 2015 while monthly means of temperature were provided in August 2016. The data

30 record was provided on a 1° equal area grid together with software to map the data onto a regular longitude and latitude grid of 1°x1°.

NVAP-M Climate / NVAP-M Ocean

The NASA Water Vapor Project (NVAP) – Making Earth System Data Records for Use in Research Environments (NVAP-M) data record was released in April 2013 (doi: 10.5067/NVAP-M/NVAP_CLIMATE_Total-Precipitable-Water_L3.001) and completely replaces the heritage NVAP data set created in the 1990's. It was created from polar orbiter satellite data along with radiosondes and surface-based Global Positioning System measurements. Further details and first results from

5 evaluation can be found in Vonder Haar et al. (2012). It contains three data types oriented towards different users: "Climate" strives for maximum temporal consistency (here: NVAP-M), "weather" strives for maximum spatial and temporal coverage and "Ocean" is a microwave-only record over the ocean (here: NVAP-O). NVAP-M and NVAP-O have a grid resolution of 1°x1°, are provided as daily averages and cover the period 1988-2009. Both contain TCWV while NVAP-M also contains layered precipitable water vapour at 4 layers. The profile data is not part of the G-VAP data archive because it is not a

10 product defined at vertical levels. NVAP-M and NVAP-O are freely available at https://eosweb.larc.nasa.gov/project/nvap/nvap-m_table and were provided as beta-version in November and December 2012, respectively. The data has not been changed between the provision of the beta-version and the doi-referenced release.

Merged Microwave REMSS

15 The REMSS monthly merged TCWV vapour product is assembled by combining measurements from SSM/I, SSMIS, AMSR-E, WindSat, and AMSR2. The vapour algorithms for each of these instruments are very similar to the AMSR-E REMSS algorithm described above. The data from each satellite are assembled into monthly 1.0°×1.0° gridded maps with valid TCWV over the world's ice-free oceans. These maps are quality controlled to exclude grid points that are corrupted by ice or land emission. Then small offsets that are derived from comparisons with TMI (Wentz, 2015) are applied to satellite

20 with significant overlap with TMI. Note that TMI measurements are not directly included in the dataset. Then the gridded maps were combined into a single dataset, using simple averaging for months when 2 or more satellite were operating. The merged TCWV product is available (at http://www.remss.com/measurements/atmospheric-water-vapor) as gridded 1.0°×1.0° gridded maps from January 1988 to the present and is updated on a monthly basis. The TCWV data record (V7) was obtained online from http://www.remss.com/measurements/atmospheric-water-vapor/tpw-1-deg-product.html in April 2013.

SSM/I+MERIS GlobVapour

The combined SSM/I+MERIS TCWV product utilises SSM/I data on-board the DMSP satellites F13 and F14 and MERIS data from ESA's 3rd reprocessing of the MERIS level 1 archive. The TCWV product was derived on a global grid over ocean and cloud free land, with a spatial resolution of 0.5° over the ice-free ocean (SSM/I) and 0.05° over land and coastal

30 ocean (MERIS). Ocean areas with sun glint, where SSM/I observations are not available, are blended with gridded MERIS data. SSM/I and MERIS data streams are processed independently and combined afterwards, leaving the individual TCWV values and their uncertainties unchanged (see Lindstrot et al., 2014 for details). To ease utilisation, the SSM/I+MERIS product is distributed on a 0.5°×0.5° grid, with the MERIS product being averaged to match the lower spatial resolution. Upon request, the product can also be provided in 0.05°×0.05° spatial resolution by oversampling the SSM/I product. The

product is available as daily composite and monthly mean and covers the period 2003 – 2008. The data record is doi-referenced (http://dx.doi.org/10.5676/DFE/WV_COMB/FP) and accessible via http://globvapour.info/products.html#daftp. The SSM/I+MERIS data record (version 1) was downloaded in January 2014.

5   TMI

TMI brightness temperature data files were obtained from NASA Goddard and were reverse engineered back to raw radiometer counts. Using a consistent processing scheme and a robust radiative transfer model, the TMI data were intercalibrated with other microwave radiometers, brightness temperatures were computed, and then the ocean measurement products were generated for distribution. This carefully applied intercalibration yields consistent products from all 10 microwave radiometer data processed at RSS. Besides TCWV the data record contains sea surface temperature, 10 m surface wind speed, 10 m surface wind speed, cloud liquid water, and rain rate. Further details are given in Wentz (1997, 2015). The data record is available at a grid resolution of 0.25°×0.25° and covers the period 7 December 1997 to 31 December 2014. The TCWV data record (V7) was obtained online from http://www.remss.com/missions/tmi.html in March 2015.

4.2 Processing

15 After download of the data records with technical specifications as described in the previous section and prior to further processing fill values, missing values and values that are outside the data record specific validity range were assigned a unique undefined value.

In order to ease joined analyses the data records are regridded onto a common grid. The data records are provided as monthly means. All data records except NVAP-M and NVAP-O are available as monthly means. NVAP-M and NVAP-O contain 20 daily averages and the daily values within a month and are arithmetically averaged using all valid observations to compute monthly means. The common grid was defined as the minimum integer multiple applicable to most of the data record grids which leads to a grid resolution of 2°x2° longitude/latitude. In order to remove a shift in the spatial grid between the satellite-based products and the reanalysis products, the reanalysis grids are shifted by half a grid box. Therefore, the CFSR, ERA-Interim, ERA-20C, JRA-55, MERRA and MERRA-2 monthly means are linearly interpolated to a grid with unchanged 25 spatial resolution but changed center positions. This approach was also applied to AMSR-E JAXA. Then, all data records are arithmetically averaged onto the common grid by considering all valid observations within a grid cell (see also Schröder et al., 2016). Note that the regridding procedure impacts the data record's internal variance and characteristics of extremes.

Some reanalysis products contain valid values below surface pressure. Thus, a common surface pressure mask was applied to all data records. The common surface pressure mask is computed on monthly basis from MERRA monthly mean surface 30 pressure, interpolated to common grid. Data below surface pressure are set to the undefined value. In case information on surface pressure is an integral part of the individual data record both masks were applied. Data at four standard pressure levels are provided: 300 hPa, 500 hPa, 700 hPa, and 1000 hPa. An interpolation was not required because in principle all

profile data records include these four levels. Note that levels are not present in nnHIRS and some reanalysis products if the level is below surface, e.g. in presence of mountains.

All data records are provided as Network Common Data Format files (http://www.unidata.ucar.edu/software/netcdf/). The data files conform to the NetCDF Climate and Forecast Metadata Convention version 1.5 (http://cf-pcmdi.llnl.gov/). In

5 addition to either TCWV (in kg/m^2), specific humidity (g/kg) or temperature (K) data, the longitude and latitude values are part of each file and defined at grid center. For the profile data records the pressure vector (in hPa) is included as well.

4.3 Archive structure

The G-VAP data archive contains TCWV as well as profiles of specific humidity and temperature. For TCWV two different versions are provided: In order to allow a joint analysis using all data records from the archive the maximum common period

10 covered by all data records was identified which is the period from January 2003 – December 2008. In order to also provide data records that allow an analysis and intercomparison of data records in climate context, a second set of data records was defined which spans the period January 1988 – December 2008 by looking for a maximum in common temporal coverage and a maximum in number of available number data records. The common period for the water vapour and temperature profile data records goes from January 1988 to December 2009. Thus the G-VAP data archive consists of four folders: 22

15 TCWV data records covering the period 2003-2008, 11 TCWV data records covering the period 1988-2008, as well as seven specific humidity and seven temperature data records covering the period 1988-2009. An overview of the folders is given in Table 3. The file names contain information on parameter, key sensor, data record name, data record version, period and G-VAP data archive version (v1.0).

Besides the cautionary note on the impact of regridding on variability of each data record the following comments need to be

20 taken into account when working with the G-VAP data archive: The data records have been downloaded between 2012 and 2016. In the meantime new data record versions of the individual elements of the archive might be available. Lastly, individual data records differ in terms of spatial and temporal sampling, coverage, and masks applied.

5 Results from intercomparison

In order to give an example of the potential analysis possible with this archive and to reveal and partly explain differences

25 among the data records, results from the intercomparison of TCWV data records over the period January 2003 – December 2008, i.e., data records from the folder TCWV/short were utilised, are shown in this section. This way all elements of the G-VAP data archive are considered in this intercomparison effort (see Table 3). The intention of this effort is to showcase differences among the data records and not to characterise uncertainties. Intercomparison results for long-term data records and for profile data records are given in Schröder et al. (2016) and Schröder et al. (2017a,b).

30 The analysis was carried out on the basis of monthly means on a regular latitude longitude grid with 2° resolution. The ensemble mean, the difference and the absolute and relative standard deviation were computed using all valid observations at

each grid point and data from all records of the G-VAP data archive. The relative standard deviation was normalised using the ensemble mean.

Figure 1 shows the ensemble mean and respective absolute and relative standard deviations based on the 22 data records. As not all data records provide global coverage the available number of data records differs regionally. Standard deviations are

5 generally lowest over ocean areas, whereas over land the values are generally larger. Regional maxima in standard deviation occur over central Africa, the tropical warm pool and South America. Largest relative standard deviations are found in polar and high mountain regions (>25%).

The intercomparison is further refined by dividing the 22 data records into the following three classes: clear-sky, cloudy-sky and all-sky. The assignment of a data record to one of these classes is done according to the predominant condition required

10 for retrieval application. Some data records include observations under predominant clear-sky conditions while others include observations under predominant clear-sky and cloudy-sky conditions as well as under all-sky conditions, i.e., additionally in presence of strong precipitation. The clear-sky class is further divided into data records which allow observations on global scales and above land only. Note that the monthly mean products have been used without any effort to harmonise the cloud and precipitation screening and that the separation of the data records according to predominant

15 condition of retrieval applicability essentially also separates the data records from different sensor types. For simplicity the terms clear-sky, cloudy-sky and all-sky class are used to indicate the predominant condition of retrieval applicability.

Figure 2 depicts ensemble means and respective standard deviations for the three different classes defined above. The all-sky class includes six data records, of which all are reanalysis products (CFSR, ERA-Interim, ERA-20C, JRA-55, MERRA, and MERRA-2). The differences among them are generally low, with absolute (relative) standard deviations values staying

20 below 3 kg/m² (15%). Largest differences are found over land areas, in particular over Africa. The cloudy-sky class includes mainly products based on passive microwave radiometers with retrieval schemes mostly limited to ice-free ocean areas: AMSR-E JAXA, AMSR-E REMSS, ATOVS, EMiR, HOAPS, NVAP-M, NVAP-O, SSMI+MERIS, Merged Microwave REMSS, and TMI. The data records agree generally well with values below 10% over large parts of the ocean, except for the polar (ocean) regions were standard deviation values larger than 25% are found. The clear-sky class includes data records

25 based on measurements from ultraviolet/visible/near-infrared imagers that cannot see through clouds and are therefore predominantly limited to clear-sky condition: AIRWAVE, HIRS UWisconsin, GOME/SCIAMACHY/GOME-2 GlobVapour, MODIS AQUA, MERIS GlobVapour, nnHIRS, and SSMI+MERIS. These data records exhibit global coverage, except AIRWAVE (ocean only) and MERIS-related products (land only). HIRS UWisconsin, GOME/SCIAMACHY/GOME-2 GlobVapour, MODIS AQUA, and nnHIRS have global coverage. Results are presented

30 separately for all data records with global coverage (third row in Figure 2) and all data records with coverage over land areas (fourth row in Figure 2). The results reveal large standard deviations between the data records both over land and ocean. Large relative standard deviations are again found over the polar region both over land and ocean. The area of the ITCZ, deserts (e.g., Sahara) and mountain regions are affected by large differences. Systematic differences might occur in mountain regions due to differences in original spatial resolution. In addition, the treatment of topography differs between the data

records and over land the ambiguity between surface properties and near surface atmospheric properties in retrieving humidity at near surface layers is challenging and differences in its treatment contribute to the observed features over land.

In order to investigate in more detail which data records cause the different areas with increased standard deviation values the difference relative to the ensemble mean was calculated for each of the 22 data records. The corresponding maps are

5   shown in Figure 3. All IR-based retrievals (AIRWAVE, HIRS UWisconsin, nnHIRS, MODIS AQUA) exhibit large positive differences over subtropical high pressure zones. GOME/SCIAMACHY/GOME-2 GlobVapour also exhibits a feature in this area but shows negative differences, thus lower values than the other IR-based retrievals. ATOVS and MERRA-2 exhibit positive differences over all continents while nnHIRS shows generally negative differences over land. On regional scale over land ERA-20C and nnHIRS show largest negative differences whereas ATOVS, MODIS AQUA and NVAP-M show largest

10   positive differences on regional scale over land. These regional scales are mainly located in the tropics, i.e., over central Africa and South America and the Sahara desert. Here also the reanalysis data records differ with ERA-20C and JRA-55 showing lower values compared to the other reanalyses. Over the ocean areas differences are generally small for all microwave based and reanalysis products except ERA-20C, JRA-55, and NVAP-O which show relatively large negative (reanalyses) and positive (NVAP-O) differences in the tropics. The features over South America, central Africa, Sahara and

15   the tropical warm pool cannot be explained by contributions from a single outlier. Schröder et al. (2016) analysed anomaly differences over the regions central Africa, Sahara and South America using a subset of data records. Their Figure 5 shows that CFSR (Sahara), MERRA (central Africa, Sahara) and NVAP-M (central Africa) exhibit break points in and opposed temporal changes (South America) over the period 2003-2008. Thus, not systematic differences but break points and opposed temporal changes can at least partly explain the distinct features at regional scale.

20   Figure 4 shows time series of TCWV and TCWV anomalies for the tropical ocean with the data records grouped according to the three different classes of predominant retrieval condition. They served to investigate the consistency of the temporal variability as possible source for differences found between the data records and to assess the presence of systematic differences among the three classes. The reanalysis data (all-sky class) show good agreement over time over the tropical ocean area with a spread of around 2 kg/m² among the different data records. This is not too surprising as the spatial maps

25   already showed the good agreement among the reanalyses over ocean. For the two other classes, however, we found areas of larger differences in Figure 2. Accordingly, relatively large spreads among the data records in the order of 5 kg/m² and 6 kg/m² for the cloudy-sky and clear-sky classes were found, respectively. Concerning the data records from the cloudy-sky class the spread is mainly caused by NVAP-O and NVAP-M which both show larger values than the others which actually agree within 2 kg/m². Despite the offsets between the data records the anomalies agree well between the data records from

30   the cloud-sky class. Only the EMiR anomalies exhibit individual months with larger differences (~1 kg/m²) in 2005 and 2006 with respect to the other anomaly time series. For the data records from the clear-sky class an offset between the individual records and differences with respect to the seasonal cycle and its magnitude were found. GOME/SCIAMACHY/GOME-2 GlobVapour and MODIS AQUA show pronounced biannual cycles with maxima in spring and fall. Reasonable agreement is found between GOME/SCIAMACHY/GOME-2 GlobVapour and AIRWAVE as well as

HIRS UWisconsin, MODIS and nnHIRS until end of 2006. Afterwards this agreement disappears. This is partly due to a small increase in TCWV for HIRS UWisconsin over the period 2003-2008 and to a decrease in TCWV for GOME/SCIAMACHY/GOME-2 GlobVapour occurring in late 2006 and 2007. The latter change coincides with the launch of Metop-A end of 2006 with the GOME-2 instrument onboard.

5   Frequently observed regional maxima in standard deviation (Figure 1 and Figure 2) and in absolute difference (Figure 3) occur in regions with persistent and large mean cloud cover. Sohn and Bennartz (2008) argue that the specific humidity (and with this TCWV) within clouds is generally larger than in surrounding clear-sky areas. This clear-sky bias is in order of 10% (Sohn and Bennartz, 2008). This is similar to the difference between HIRS UWisconsin, MODIS AQUA, and nnHIRS and AMSR-E JAXA, AMSR-E REMSS, ATOVS, HOAPS, Merged Microwave REMSS and TMI REMSS (Figure 4). However,

10 the variability in TCWV within the cloudy-sky and the clear sky class is relatively large (Figure 4) and prohibits conclusions on systematic differences between the all-sky and cloudy-sky as well as between the cloudy-sky and clear-sky class. It is recalled that the presented results are based on a separation of the data records according to predominant retrieval condition and not according to atmospheric condition.

6 Data availability

15 The G-VAP data archive was generated in April 2017. The data is available in netCDF format and can be accessed via http://dx.doi.org/10.5676/EUM_SAF_CM/GVAP/V001 (Schröder et al., 2017c).

7 Conclusions

An overview of satellite sensors capable of retrieving quantitative information on atmospheric water vapour and of available water vapour data records based on satellite observations and reanalyses is given. The summary tables on available data

20 records include information on technical specifications such as coverage and resolution in order to allow a first order decision on utilisation by a user. 22 data records remain after restricting the temporal coverage to a minimum of 10 years. These data records are described in some more details on methodology and basic technical specifications and form the basis of the G-VAP data archive. The archive contains profiles of temperature in K (1988-2009) and of specific humidity in g/kg (1988-2009), long-term TCWV (1988-2008) and short-term TCWV (2003-2008), both in kg/m^2. All data records have been

25 regridded onto a common regular longitude/latitude grid with 2° spatial resolution. The profile data records contain information at 4 levels: 1000, 700, 500 and 300 hPa. The G-VAP data archive is freely available at http://dx.doi.org/10.5676/EUM_SAF_CM/GVAP/V001 and includes the vast majority of available water vapour data records from satellite and reanalyses with a temporal coverage of at least 10 years. The G-VAP data archive is designed to allow direct intercomparisons using a subset of or the full archive. Except for analysis which requires a high level of stability

the archive can be used in context of climate analysis, climate model evaluation and the analysis of impacts and dynamics associated to large scale climate relevant phenomena such as El Nino.

In order to give an example of the potential analysis possible with this archive and to showcase differences among the data records, TCWV data records over the period January 2003 – December 2008 were intercompared. This way all 22 elements

5 of the G-VAP data archive are considered. The intercomparison revealed regions of distinct differences among the data records: central Africa, tropical warm pool, South America, as well as polar and mountain regions. To further refine the analysis the data records were separated into three classes of predominant condition of retrieval applicability: all-sky, cloudy-sky and clear-sky. The spread of the time series' in each class can be large and exceeds the differences between the classes. Also, the separation into the three classes essentially also separates the data records from sensor types. Thus,

10 conclusions on systematic differences between the classes can not be drawn.

G-VAP will continue to work on the characterisation of water vapour data records. In particular, new data records and updated versions of already analysed data records will be implemented into future versions of the G-VAP data archive in order to continue to strive for completeness and in order to describe changes in quality between the different versions.

Appendix A

15 This appendix gives definitions for the abbreviations that are used in this paper.

Competing interests

The authors declare that they have no conflict of interest.

Acknowledgment

The work done by M. Lockhoff and M. Schröder was performed within the EUMETSAT CM SAF framework. They

20 acknowledge the financial support of the EUMETSAT member states. Informus GmbH was funded under ESA's Long-Term Data Preservation program. I. Sommerfeld supported the editing process. The AIRWAVE v1 dataset was developed with the financial support of the ESA's Long-Term Data Preservation ATSR Long Term Stability Project. ERA-20C was funded by the European Union FP-7 project ERA-CLIM (grant agreement number 265229). MERRA-2 development support is provided by the NASA Modeling, Analysis and Prediction program.

25 **References**

Andersson, A., Fennig, K., Klepp, C., Bakan, S., Graßl, H., and Schulz, J.: The Hamburg Ocean Atmosphere Parameters and Fluxes from Satellite Data – HOAPS-3, Earth Syst. Sci. Data, 2, 215–234, doi:10.5194/essd-2-215-2010, 2010.

Bauer, P., Lopez, P., Benedetti, A., Salmond, D., Moreau, E.: Implementation of 1D+4D-Var assimilation of precipitation-affected microwave radiances at ECMWF. I: 1D-Var, Q. J. R. Meteorol. Soc. 132: 2277–2306, 2006a.

5   Bauer, P., Lopez, P., Salmond, D., Benedetti, A., Saarinen, S., Moreau, E.: Implementation of 1D+4D-Var assimilation of precipitation-affected microwave radiances at ECMWF. II: 4D-Var, Q. J. R. Meteorol. Soc. 132: 2307–2332, 2006b.

Bennartz, R., Höschen, H., Picard, B., Schröder, M., Stengel, M., Sus, O., Bojkov, B., Casadio, S., Diedrich, H., Eliasson, S., Fell, F., Fischer, J., Hollmann, R., Preusker, R. and Ulrika, W.: An intercalibrated dataset of Total Column Water Vapour
10   and Wet Tropospheric Correction based on MWR on board ERS-1, ERS-2 and Envisat, Atmos. Meas. Tech., 10, 1387-1402, doi:10.5194/amt-10-1387-2017, 2017.

Borbas, E., Seemann, S. W., Huang, H.-L., Li, J., and Menzel, W. P.: Global profile training database for satellite regression retrievals with estimates of skin temperature and emissivity, Proc. of the Int. ATOVS Study Conference-XIV, Beijing,
15   China, 25-31 May 2005, pp. 763-770, Available at: https://cimss.ssec.wisc.edu/itwg/itsc/itsc14/proceedings/B32_Borbas.pdf, 2005.

Bosilovich, M.G., Robertson, F.R., Takacs, L., Molod, A. and Mocko, D.: Atmospheric Water Balance and Variability in the MERRA-2 Reanalysis. J. Climate, 30, 1177–1196, https://doi.org/10.1175/JCLI-D-16-0338.1, 2017.

Bouffies, S., Breon, F. M., Tanre, D. and Dubuisson, P., Atmospheric water vapor estimate by a differential absorption technique with the polarization and directionality of the Earth reflectances (POLDER) instrument. Geophys. Res. Let., 102, 3831-3841, 1997.

25   Boukabara, S.-A., and 12 co-authors: MiRS: An All-Weather 1DVAR Satellite Data Assimilation and Retrieval System, IEEE Trans, Geosci. Remote Sens., 49 (9), pp. 3249-3272, doi:10.1109/TGRS.2011.2158438, 2011.

Casadio, S., Castelli, E., Papandrea, E., Dinelli, B. M., Pisacane, G., Burini, A., Bojkov , B. R.: Total column water vapour from along track scanning radiometer series using thermal infrared dual view ocean cloud free measurements: The Advanced
30   Infra-Red WAter Vapour Estimator (AIRWAVE) algorithm, Remote Sensing of Environment 172 (2016) 1–14, http://dx.doi.org/10.1016/j.rse.2015.10.037

Castelli, E., Casadio, S., Papandrea, E., Dinelli, B. M., Burini, A., and Bojkov, B.: Total Column Water Vapour from Along Track Scanning Radiometer Series: Advanced Infra-Red Water Vapour Estimator (AIRWAVE) algorithm description and

applications, S3forScience2015, 2-5 June 2015, Venice, Italy, http://seom.esa.int/S3forScience2015/page_session14.php, 2015.

Chahine, M. T., Pagano, T. S., Aumann, H. H., Atlas, R., Barnet, C., Blaisdell, J., Chen, L., Divakarla, M., Fetzer, E. J., Goldberg, M., Gautier, C., Granger, S., Hannon, S., Irion, F. W., Kakar, M., Kalnay, E., Lambrigsten, B. H., Lee, S.-Y., Le Marshall, J., McMillan, W. W., McMillin, L., Olsen, E. T., Revercomb, H., Rosenkranz, P., Smith, W. L., Staelin, D., Larrabee Strow, L., Susskind, J., Tobin, S., Wolf, W. and Zhou, L.: AIRS: Improving weather forecasting and providing new data on greenhouse gases, Bull. Amer. Meteor. Soc., 87, 911-926, doi:10.1175/bams-87-7-911, 2006.

Chung, E.-S., Soden, B. J., and John, V. O.: Intercalibrating Microwave Satellite Observations for Monitoring Long-Term Variations in Upper- and Midtropospheric Water Vapor, J. Atmos. Oceanic Technol., 30, 2303–2319. DOI: 10.1175/JTECH-D-13-00001.1, 2013.

Clayson, C. A., Roberts, J. B., and Bogdanoff, A. S.: The SeaFlux Turbulent Flux dataset version 1.0 documentation, SeaFlux Project, 5pp. [available online at http://seaflux.org/seaflux_data/DOCUMENTATION/SeaFluxDocumentationV12.pdf], 2012.

Courcoux, N. and Schröder, M.: The CM SAF ATOVS data record: overview of methodology and evaluation of total column water and profiles of tropospheric humidity, Earth Syst. Sci. Data, 7, 397-414, doi:10.5194/essd-7-397-2015, 2015.

Cram, T. A., and coauthors: The International Surface Pressure Databank version 2, Geosci. Data J., 2, 31–46, doi:10.1002/gdj3.25, 2015.

Davis, S., and Rosenlof, K.: NOAA ESRL Stratospheric Water and OzOne Satellite Homogenized (SWOOSH), Version 2, NOAA National Centers for Environmental Information (NCEI). doi:10.7289/V5TD9VBX, 2016.

Dee, D. P. and 35 co-authors: The ERA-Interim reanalysis: Configuration and performance of the data assimilation system, Quart. J. R. Meteorol. Soc., 137, 553-597, doi:10.1002/qj.828, 2011.

Du, J., Kimball, J. S. and Jones, L. A.: Satellite microwave retrieval of total precipitable water vapor and surface air temperature over land from AMSR2, IEEE Trans. Geosci. Remote Sens., 53(5): 2520-2531, 2015.

Fennig, K., Andersson, A., Schröder, M.: Fundamental Climate Data Record of SSM/I / SSMIS Brightness Temperatures. Satellite Application Facility on Climate Monitoring, DOI:10.5676/EUM_SAF_CM/FCDR_MWI/V002. http://dx.doi.org/10.5676/EUM_SAF_CM/FCDR_MWI/V002, 2015.

5   Forsythe, J. M., Kidder, S. Q., Fuell, K. K., LeRoy, A., Jedlovec, G. J., and Jones, A. S.: A multisensor, blended, layered water vapor product for weather analysis and forecasting, J. Operational Meteor., 3 (5), 41–58. doi: http://dx.doi.org/10.15191/nwajom.2015.0305, 2015.

Gao, B.-C. and Kaufman, Y. J.: Water vapor retrievals using Moderate Resolution Imaging Spectroradiometer (MODIS)
10   near-infrared channels, J. Geophys. Res.-Atmos., 108, 4389, doi:10.1117/12.154909, 2003.

Gelaro, R., and co-authors: The Modern-Era Retrospective Analysis for Research and Applications, Version 2 (MERRA-2). J. Climate, 30, 5419–5454, https://doi.org/10.1175/JCLI-D-16-0758.1, 2017

15   Grossi, M., Valks, P., Loyola, D., Aberle, B., Slijkhuis, S., Wagner, T., Beirle, S. and Lang, R.: Total column water vapour measurements from GOME-2 MetOp-A and MetOp-B, Atmos. Meas. Tech., 8(3), 1111-1133, doi:10.5194/amt-8-1111-2015, 2015.

Healy, S. B. and Eyre, J. R.: Retrieving temperature, water vapour and surface pressure information from refractive-index
20   profiles derived by radio occultation: A simulation study. Q. J. R. Meteorol. Soc., 126, 1661–1683. doi: 10.1002/qj.49712656606, 2010.

Held, I. M. and Soden, B. J.: Water vapour feedback and global warming, Annu. Rev. Energ. Env., 25, 441–475, 2000.

25   Hersbach, H., Peubey, C., Simmons, A., Berrisford, P., Poli, P. and Dee, D. P.: ERA-20CM: A twentieth century atmospheric model ensemble, Quart. J. Roy. Meteor. Soc., 141, 2350–2375, doi:10.1002/qj.2528, 2015.

Hersbach, H., and Dee, D.: ECMWF Newsletter, 147, page 7, 2016.

30   Hilburn, K. A. and Wentz, F. J.: Intercalibrated Passive Microwave Rain Products From the Unified Microwave Ocean Retrieval Algorithm (UMORA), J. Appl. Meteor. Climatol., 47, 778-794, doi:10.1175/2007JAMC1635.1, 2008.

Geer, A. J., Bauer, P., and Lopez, P.: Lessons learnt from the operational 1D+4D-Var assimilation of rain- and cloud-affected SSM/I observations at ECMWF. Q. J. R. Meteorol. Soc., 134, 1513–1525, 2008.

John, V. O., Holl, G., Buehler, S. A., Candy, B., Saunders, R. W., and Parker, D. E.: Understanding intersatellite biases of microwave humidity sounders using global simultaneous nadir overpasses, J. Geophys. Res., 117, D02305, doi:10.1029/2011JD016349, 2012.

Kahn, B. H., Irion, F. W., Dang, V. T., Manning, E. M., Nasiri, S. L., Naud, C. M., Blaisdell, J. M., Schreier, M. M., Yue, Q., Bowman, K. W., Fetzer, E. J., Hulley, G. C., Liou, K. N., Lubin, D., Ou, S. C., Susskind, J., Takano, Y., Tian, B., and Worden, J. R.: The Atmospheric Infrared Sounder version 6 cloud products, Atmos. Chem. Phys., 14, 399-426, https://doi.org/10.5194/acp-14-399-2014, 2014.

Kämpfer, N., Ed.: Monitoring Atmospheric Water Vapour: Ground-Based Remote Sensing and In-situ Methods, series: ISSI Scientific Report, edition: 10, Springer New York, 2012, ISBN 978-1-4614-3908-0, 2012.

Kazumori, M.: Description of GCOM-W1 AMSR2 Integrated Water Vapor and Cloud Liquid Water Retrieval Algorithm,

15   Chapter2 of "Descriptions of GCOM-W1 AMSR2 Level 1R and Level 2 Algorithms", Available at: http://suzaku.eorc.jaxa.jp/GCOM_W/data/doc/NDX-120015A.pdf, 2013.

Kazumori, M., Egawa T., and Yoshimoto, K.: A retrieval algorithm of atmospheric water vapor and cloud liquid water for AMSR-E. European Journal of Remote Sensing, 45, 63 – 74. doi: 10.5721/EuJRS20124507, 2012.

Kobayashi, S. and 11 co-authors: The JRA-55 Reanalysis: General Specifications and Basic Characteristics, J. Met. Soc. Jap., 93(1), 5-48, doi:10.2151/jmsj.2015-001, 2015.

Kursinski, E. R., and Gebhardt, T.: A method to deconvolve errors in GPS RO-derived water vapor histograms, J. Atmo.

25   Ocean. Tech., 31(12), 2606-2628, 2014.

Kursinski, E. R., Hajj, G. A., Schofield, J. T., Linfield, R. P., and Hardy, K. R.: Observing Earth's atmosphere with radio occultation measurements using the Global Positioning System., J. Geophys. Res.: Atmo. (1984–2012), 102.D19, 23429-23465. DOI: 10.1029/97JD01569, 1997.

Li, J., Wolf, W. W., Menzel, W. P., Zhang, W., Huang, H.-L. and Achtor, T. H.: Global Soundings of the Atmosphere from ATOVS Measurements: The Algorithm and Validation, J. Appl. Meteor., 39, 1248–1268, 2000.

Lindstrot, R., Preusker, R., Diedrich, H., Doppler, L., Bennartz, R., and Fischer, J.: 1D-Var retrieval of daytime total columnar water vapour from MERIS measurements, Atmos. Meas. Tech., 5, 631–646, doi:10.5194/amt-5-631-2012, 2012.

Lindstrot, R., Stengel, M., Schröder, M., Fischer, J., Preusker, R., Schneider, N., Steenbergen, T., and Bojkov, B.: A global
5   climatology of total columnar water vapour from SSM/I and MERIS, Earth Syst. Sci. Data, 6, 221–233, 2014, www.earth-syst-sci-data.net/6/221/2014/, doi:10.5194/essd-6-221-2014, 2014.

Mears, C. A., Wang, J., Smith, D. and Wentz, F. J.: Intercomparison of Total Precipitable Water Measurements Made by Satellite-Borne Microwave Radiometers and Ground-Based GPS Instruments, Journal of Geophysical Research:
10   Atmospheres, 120(6), 2492-2504, doi:10.1002/2014JD022694, 2015.

Meissner, T., and Wentz, F. J.: The emissivity of the ocean surface between 6 - 90 GHz over a large range of wind speeds and Earth incidence angles, IEEE Transactions on Geoscience and Remote Sensing, 50(8), 3004-3026, 2012.

15   Nelson, R. R., Crisp, D., Ott, L. E., and O'Dell, C. W., High-accuracy measurements of total column water vapor from the Orbiting Carbon Observatory-2, Geophys. Res. Lett., 43, 12,261–12,269, doi:10.1002/2016GL071200, 2016.

Noël, S., Buchwitz, M. and Burrows, J. P., First retrieval of global water vapour column amounts from SCIAMACHY measurements, Atmos. Chem. Phys., 4, 111-125, 2004.

Platnick, S., Hubanks, P., Meyer, K., and King, M. D.: MODIS Atmosphere L3 Monthly Product (08_L3). NASA MODIS Adaptive Processing System, Goddard Space Flight Center, http://dx.doi.org/10.5067/MODIS/MOD08_M3.006 (Terra), http://dx.doi.org/10.5067/MODIS/MYD08_M3.006 (Aqua), 2015.

25   Poli, P. and 14 co-authors: ERA-20C: An Atmospheric Reanalysis of the Twentieth Century, J. Climate, 29, 4083–4097, doi:10.1175/JCLI-D-15-0556.1, 2016.

Reichle, R., Liu, Q., Koster, R., Draper, C., Mahanama, S. and Partyka, G.: Land Surface Precipitation in MERRA-2. J. Clim. doi:10.1175/JCLI-D-16-0570.1, 2017.

Rienecker, M. M. and 28 co-authors: MERRA: NASA's Modern-Era Retrospective Analysis for Research and Applications, J. Climate, 24, 3624–3648, doi:10.1175/JCLI-D-11-00015.1, 2011.

Rossow, W.B., and Pearl, C.: New atmospheric temperature-humidity profile data product, J. Atmos. Ocean Tech., submitted, 2017.

Saha, S. and 51 co-authors: The NCEP Climate Forecast System Reanalysis, Bull. Amer. Meteor. Soc., 91, 1015–1057, doi:10.1175/2010BAMS3001.1, 2010.

Sapiano, M. R. P, Berg, W. K., McKague, D. S. and Kummerow, C. D.: Towards an intercalibrated fundamental climate data record of the SSM/I sensors, IEEE Trans. Geocsi. And Rem. Sens., 51, 1492-1503, 2013.

Scott, N. A. and 8 co-authors: Characteristics of the TOVS Pathfinder Path-B dataset, Bull. Am. Meteorol. Soc., 80, 2679–2701, doi:10.1175/1520-0477(1999)080%3C2679:COTTPP%3E2.0.CO;2, 1999.

Schlüssel, P. and Emery, W. J.: Atmospheric water vapour over oceans from SSM/I measurements, Int. J. Remote Sens., 11, 753–766, 1990.

Schröder, M., Lockhoff, M., Forsythe, J., Cronk, H., Vonder Haar, T. H., Bennartz, R.: The GEWEX water vapor assessment (G-VAP) – results from the trend and homogeneity analysis, J. Applied Meteor. Clim., 1633-1649, 55 (7), doi:10.1175/JAMC-D-15-0304.1, 2016.

Schröder, M., Lockhoff, M., Shi, L., August, T., Bennartz, R., Borbas, E., Brogniez, H., Calbet, X., Crewell, S., Eikenberg, S., Fell, F., Forsythe, J., Gambacorta, A., Graw, K., Ho, S.-P., Höschen, H., Kinzel, J., Kursinski, E. R., Reale, A., Roman, J., Scott, N., Steinke, S., Sun, B., Trent, T., Walther, A., Willen, U., Yang, Q.: GEWEX water vapor assessment (G-VAP) - Final Report. Submitted to GDAP for publication as WCRP report, 2017a.

Schröder, M., Lockhoff, M., Shi, L., August, T., Bennartz, R., Calbet, X., Fell, F., Forsythe, J., Gambacorta, A., Ho, S.-P., Kursinski, E. R., Reale, A., Trent, T., Yang, Q.: The GEWEX water vapor assessment of global water vapour and temperature data records from satellites and reanalyses. In preparation for submission to BAMS, 2017b.

Schröder, M., M. Lockhoff, F. Fell, J. Forsythe, T. Trent, R. Bennartz, E. Borbas, M. G. Bosilovich, E. Castelli, H. Hersbach, M. Kachi, S. Kobayashi, D. Loyola, C. Mears, R. Preusker, W. B. Rossow, S. Saha: The GEWEX Water Vapor Assessment archive of water vapour products from satellite observations and reanalyses, DOI: 10.5676/EUM_SAF_CM/GVAP/V001, http://dx.doi.org/10.5676/EUM_SAF_CM/GVAP/V001, 2017c.

Seemann, S. W., Borbas, E. E., Knuteson, R. O., Stephenson, G. R., and Huang, H.-L.: Development of a global infrared emissivity database for application to clear-sky sounding retrievals from multi-spectral satellite radiances measurements, J. Appl. Meteor. and Clim., 47, 108-123, doi:10.1175/2007JAMC1590.1, 2008.

5   Seemann, S. W., Li, J., Menzel, W. P., and Gumley, L. E.: Operational retrieval of atmospheric temperature, moisture, and ozone from MODIS infrared radiances, J. Appl. Meteor., 42, 1072-1091, doi:10.1175/1520-0450(2003)042%3C1072:OROATM%3E2.0.CO;2, 2003.

Shi, L., Bates, J. J., and Cao, C.: Scene Radiance–Dependent Intersatellite Biases of HIRS Longwave Channels, J. Atmos.
10 Ocean. Tech., 25, 2219–2229, doi:10.1175/2008jtecha1058.1, 2008.

Shi, L., Matthews, J., Ho, S.-P., Yang, Q., and Bates, J.: Algorithm Development of Temperature and Humidity Profile Retrievals for Long-Term HIRS Observations, Remote Sensing, 8, 280, doi:10.3390/rs8040280, 2016.

15 Smith, A., Lott, N., and Vose, R.: The Integrated Surface Database: Recent developments and partnerships. Bull. Amer. Meteor. Soc., 92, 704-708, doi:10.1175/2011BAMS3015.1, 2011.

Sohn, B. J., and Bennartz, R.: Contribution of water vapor to observational estimates of longwave cloud radiative forcing. J. Geophys. Res., 113, D20107, doi:101029/2008JD010053, 2008.

Stubenrauch, C. J., Rossow, W. B., Kinne, S., Ackerman, S., Cesana, G., Chepfer, H., Di Girolamo, L., Getzewich, B., Guignard, A., Heidinger, A., Maddux, B., Menzel, P., Minnis, P., Pearl, C., Platnick, S., Poulsen, C., Riedi, J., Sun-Mack, S., Walther, A., Winker, D., Zeng, S., Zhao, G.: Assessment of global cloud datasets from satellites: Project and Database initiated by the GEWEX Radiation Panel, Bull. Amer. Meteor. Soc., doi: 10.1175/BAMS-D-12-00117, 2012.

Susskind, J., Piraino, P., Rokke, L., Iredell, L., and Mehta, A.: Characteristics of the TOVS Pathfinder Path A data set, Bull. Am. Meteorol. Soc., 78(7), 1449-1472, doi:10.1175/1520-0477(1997)078<1449:COTTPP>2.0.CO;2, 1977.

Takacs, L. L., Suarez, M. and Todling, R.: Maintaining atmospheric mass and water balance in reanalyses. Quart. J. Roy.
30 Meteor. Soc., 142, 1565–1573, doi:https://doi.org/10.1002/qj.2763, 2016.

Takeuchi, Y.: Algorithm theoretical basis document (ATBD) of the algorithm to derive total water vapor content from ADEOS-II/AMSR. EORC Bulletin/Technical Report, Special Issue on AMSR Retrieval Algorithms, Available at: http://sharaku.eorc.jaxa.jp/AMSR/products/pdf/alg_des.pdf, 2002.

Takeuchi, Y., Tauchi, T., Saito, S., Imaoka, K., Kachi, M., and Shibata, A.: A total column precipitable water algorithm for ADEOS-II/AMSR and Aqua/AMSR-E. Italian Journal of Remote Sensing 30/31, 143 –157, 2004.

5   Taylor, K., Stouffer, R. and Meehl, G.: An overview of CMIP5 and the experiment design, Bull. Amer. Meteor. Soc., 93, 485–498, doi:10.1175/BAMS-D-11-00094.1, 2012.

Trenberth, K.E., Jones, P. D., Ambenje, P., Bojariu, R., Easterling, D., Klein Tank, A., Parker, D., Rahimzadeh, F., Renwick, J. A., Rusticucci, M., Soden, B., and Zhai, P.: Observations: Surface and Atmospheric Climate Change. In: Climate Change
10 2007: The Physical Science Basis. Contribution of Working Group I to the Fourth Assessment Report of the Intergovernmental Panel on Climate Change [Solomon, S., D. Qin, M. Manning, Z. Chen, M. Marquis, K.B. Averyt, M. Tignor and H.L. Miller (eds.)]. Cambridge University Press, Cambridge, United Kingdom and New York, NY, USA, 2007.

Vonder Haar, T. H., Bytheway, J. L., and Forsythe, J. M.: Weather and climate analyses using improved global water vapor
15 observations, Geophys. Res. Lett., 39, L15802, doi:10.1029/2012GL052094, 2012.

Wagner, T., Heland, J., Zöger, M. and Platt, U.: A fast H2O total column density product from GOME – Validation with in-situ aircraft measurements, Atmos. Chem. Phys., 3(3), 651-663, doi:10.5194/acp-3-651-2003, 2003.

20 Wang, H., Gonzalez Abad, G., Liu, X., and Chance, K.: Validation and update of OMI Total Column Water Vapor product, Atmos. Chem. Phys., 16, 11379-11393, https://doi.org/10.5194/acp-16-11379-2016, 2016.

Wee, T.-K., and Kuo, Y.-H.: A perspective on the fundamental quality of GPS radio occultation data, Atmos. Meas. Techn. 8.10: 4281-4294, 2015.

Wentz, F. J.: A well-calibrated ocean algorithm for SSM/I, J. Geophys. Res., 102, 8703–8718, doi:10.1029/96JC01751, 1997.

Wentz, F. J.: A 17-yr climate record of environmental parameters derived from the Tropical Rainfall Measuring Mission
30 (TRMM) Microwave Imager, J. Climate, 28, 6882–6902, doi:10.1175/JCLI-D-15-0155.1, 2015.

Wentz, F. J., and Meissner, T.: Atmospheric absorption model for dry air and water vapor at microwave frequencies below 100 GHz derived from spaceborne radiometer observations, Radio Science 51(5), 381-391, doi:10.1002/2015RS005858, 2017.

Woodruff, S. D., and coauthors: ICOADS release 2.5: Extensions and enhancements to the surface marine meteorological archive, Int. J. Climatol., 31, 951–967, doi:10.1002/joc.2103, 2011.

5 Worden, J., and 18 co-authors, Tropospheric emission spectrometer observations of the tropospheric HDO/H2O ratio: Estimation approach and characterization, J. Geophys. Res., 111, D16309, doi:10.1029/2005JD006606, 2006.

Wulfmeyer, V., Hardesty, R. M., Turner, D. D., Behrendt, A., Cadeddu, M. P., Di Girolamo, P., Schlüssel, P.,Van Baelen, J., and Zus, F., A review of the remote sensing of lower tropospheric thermodynamic profiles and its indispensable role for the
10 understanding and the simulation of water and energy cycles, Rev. Geophys., 53, 819–895, doi:10.1002/2014RG000476, 2015.

Xie, F., Syndergaard, S., Kursinski, E. R., and Herman, B. M.: An approach for retrieving marine boundary layer refractivity from GPS occultation data in the presence of superrefraction, Journal of Atmospheric and Oceanic Technology, 23(12),
15 1629-1644, 2006.

Table 1: Summary of main satellite instruments used for water vapour climate data records. Spatial resolution is typically given at nadir. The last column provides information on the applicability of typical water vapour retrieval schemes under certain conditions and in certain regions.

Sensor	Type	Platform	Spatial	Number of channels	Spatial sampling characteristics
(A)ATSR	Visible (ATSR-2, AATSR), NIR and IR radiometer	Polar	1 km	7 (4 for ATSR-1)	clear, ocean
AIRS	Infrared Hyperspectral Sounder (spectrometer)	Polar	15 km	2378	clear, ocean+land
AMSR-E	Microwave Imager	Polar	12 km	12	clear+cloudy, ocean
AMSU-B / MHS	Microwave Sounder	Polar	15 km	5	clear+cloudy, ocean
COSMIC	GPS Radio Occultation Limb Sounding	Polar	~100 km along a ray	2	clear+cloudy, ocean+land
GOME	UV/VIS/NIR spectrometer	Polar	40 km x 320 km	3584	clear, ocean+land
GRAS	GPS Radio Occultation Limb Sounding	Polar	~100 km along a ray	2	clear+cloudy, ocean+land
HIRS	Infrared Broadband Sounder (radiometer)	Polar	20 km	20	clear, ocean+land
IASI	Infrared Hyperspectral Sounder (spectrometer)	Polar	12 km	8461	clear, ocean+land

MERIS	Visible and NIR spectrometer	Polar	1 km	15	clear, land
MODIS	Visible, NIR and IR spectro-radiometer	Polar	0.25 – 1 km	36	clear
MWR	Microwave Imager	Polar	20 km x 20 km	2	clear+cloudy, ocean
SSM/I	Microwave Imager	Polar	40 km	7	clear+cloudy, ocean
SSMIS	Microwave Imager	Polar	47 km	24	clear+cloudy, ocean
SSM/T-2	Microwave Sounder	Polar	50 km	5	clear+cloudy, ocean
TMI	Microwave Imager	Low inclination tropical orbit	10 km	9	clear+cloudy, ocean
TMR	Microwave Imager	Polar	11 km x 5 km	3	clear+cloudy, ocean

Table 2: Satellite and reanalysis data records. Typically the data record name is given under "Data record". If not available the owner's name is provided. * Element of the G-VAP data archive.

Technique	Data record	Para-meters	Spatial/temporal resolution	Spatial/temporal coverage	Reference(s)
(A)ATSR	AIRWAVE*	TCWV	1x1 km^2, 0.25°, daily	global, 11/1991 - 02/2012	Casadio et al. (2016), Castelli et al. (2015)
AIRS, HIRS, SSM/I, GNSS, Radiosondes	NVAP-M Climate*	TCWV, WV	1° or 0.5°, daily	global, 01/1988- 12/2009	10.5067/NVAP-M/NVAP_CLIMATE_Total-Precipitable-Water_L3.001, Vonder Haar et al. (2012)
AIRS, AMSU, HSB	NASA	TCWV, WV, T	1°, 12 levels, daily, monthly	global, 09/2002-present	https://airs.jpl.nasa.gov/data/algorithms
AIRS, AMSU-A, CPR, MODIS	AIRSM_CPR_IND	WV, T	45 km, daily-weekly	global, 07/2006-11/2012	https://reverb.echo.nasa.gov/reverb/
AMSR2, AMSR-E, SSM/I, SSMIS, WindSat	REMSS*	TCWV	1.0°, monthly	global ice-free ocean, 01/1988-present	Hilburn and Wentz (2008)
AMSR-E	REMSS*	TCWV	0.25°, monthly	global ocean, 06/2002-09/2011	Hilburn and Wentz (2008)
AMSR-E	JAXA*	TCWV	Level 2: sensor resolution, Level 3: 0.25°, monthly	global ocean, 06/2002-10/2011	https://gcom-w1.jaxa.jp, http://sharaku.eorc.jaxa.jp/AMSR/products/, Takeuchi (2002)
ATOVS	CM SAF*	TCWV, WV, T	90 km, daily, monthly	global, 01/1999-12/2011	10.5676/EUM_SAF_CM/WVT_ATOVS/V001, Courcoux and Schröder (2015)
COSMIC	ROM SAF	WV, T	5°, vertically 200 m, 0-12 km, monthly	global (zonal means), 05/2006-present	http://www.romsaf.org/GRM-19.php, http://www.romsaf.org/GRM-20.php, http://preop.romsaf.org/pro

					duct_documents/romsaf_atbd_1dvar.pdf
COSMIC	UCAR	WV, T	sensor resolution, vertically 100 m, sensor resolution	global, 05/2006-04/2014	http://cdaac-www.cosmic.ucar.edu/cdaac/products.html, Wee and Kuo (2015)
GOME, SCIAMACHY, GOME-2	UBremen	TCWV	sensor resolution, sensor resolution	global, 07/1995-03/2012	http://www.iup.uni-bremen.de/amcdoas/, Noel et al. (2004)
GOME, SCIAMACHY, GOME-2	GlobVapour*	TCWV	sensor resolution, 0.5°, monthly	global, 01/1996-12/2008	Grossi et al. (2015)
GRAS	UCAR	WV, T	sensor resolution, vertically 100 m, sensor resolution	global, 10/2007-12/2011	http://cdaac-www.cosmic.ucar.edu/cdaac/products.html
HIRS	nnHIRS	TCWV, WV, T	1°, 17 levels (10 hPa top) (T), 3-hourly, monthly	global, 08/1979–12/2014	Rossow and Perl (2017)
HIRS	NOAA	TCWV, WV, T	sensor resolution, 8 layers, sensor resolution	global, 07/1979-12/2014	Shi et al. (2016)
HIRS	UWisconsin*	TCWV, WV	0.5°, 3 layers (10-440 hPa top), 6-hourly, monthly	global, 07/1980–03/2016	Borbas et al. (2005), Seemann et al. (2003, 2008)
MERIS	GlobVapour*	TCWV	0.05°, 0.5°, daily, monthly	global land, 01/2003-09/2012	Lindstrot et al. (2012)
MODIS	MOD08, MYD08*	TCWV, WV	1°, 20 levels (5 hPa top), daily, monthly	global, 2000-2014 (TERRA); 2002-2014 (AQUA)	http://dx.doi.org/10.5067/MODIS/MOD08_M3.006, http://dx.doi.org/10.5067/MODIS/MYD08_M3.006, Platnick et al. (2015)
MWR	EMiR*	TCWV	0.5°, sensor resolution,	global, 08/1991-03/2012	10.5676/DWD_EMIR/V001, Bennartz et al. (2017)

monthly

OCO-2	CSU	TCWV	1.3 km x 2.3 km, sensor resolution	global, 08-2014-present	Nelson et al., 2016
OMI	NASA/Harvard	TCWV	13 km x 24 km at nadir, sensor resolution	global, 01/2005–12/2009	Wang et al. (2016)
POLDER	U Lille	TCWV	1/6°, sensor resolution, daily, monthly	global, 12/2004-12/2013	http://www.icare.univ-lille1.fr//archive/?dir=PARASOL/RB2.v18.19/, Bouffies et al. (1997)
Reanalysis	ERA-Interim*	TCWV, WV, T	~80 km (T255), 60 levels (0.1 hPa top), 6-hourly, monthly	global, 01/1979-present	Dee et al. (2011)
Reanalysis	ERA-20C*	TCWV, WV, T	~125 km (T159), 91 levels (0.01 hPa top), 3-hourly, monthly	global, 01/1900-12/2010	Poli et al. (2016)
Reanalysis	MERRA*	TCWV, WV, T	0.5° x 0.667°, 72 levels (0.01 hPa top), hourly (TCWV), 6-hourly, monthly	global, 01/1979-02/2016	Rienecker et al. (2011)
Reanalysis	MERRA-2	TCWV, WV, T	0.5° x 0.625°, 72 levels (top 0.01 hPa), hourly, 6-hourly, monthly	global, 01/1980–present	Gelaro et al. (2017)
Reanalysis	CFSR*	TCWV, WV, T	0.5° (T382), 37 levels (0.266 hPa top), hourly, monthly	global, 01/1979-present	Saha et al. (2010)
Reanalysis	JRA-55*	TCWV, WV, T	~55 km (T319) or 1.25°, 60 levels (0.1 hPa top), 3-hourly,	global, 01/1958-present	Kobayashi et al. (2015)

			6-hourly, monthly		
SSM/I	HOAPS*	TCWV	0.5°, 6-hourly, monthly	global ocean, 07/1987-12/2008	Schlüssel and Emery (1990), Andersson et al. (2010)
SSM/I	NVAP-M Ocean*	TCWV	1.0°, daily	global ice-free ocean, 01/1988-12/2009	10.5067/NVAP-M/NVAP_CLIMATE_Total-Precipitable-Water_L3.001, Vonder Haar et al. (2012)
SSM/I, MERIS	GlobVapour*	TCWV	0.05°, 0.5°, daily, monthly	global, 01/2003-12/2008	10.5676/DFE/WV_COMB /FP, Lindstrot et al. (2014)
TES	NASA	TCWV, WV, T	4° x 2°, daily, monthly	global, 09/2004-present	https://tes.jpl.nasa.gov/data Worden et al. (2006)
TMI	REMSS*	TCWV	0.25°, monthly	global ocean, 12/1997-12/2014	Wentz (1997, 2015)
TOVS	TOVS Path B	TCWV, WV, T	1°, 4 layers (300 hPa top), daily, monthly	global, 01/1987-06/1995	Scott et al. (1999)
TOVS	TOVS Path A	TCWV, WV, T	1°, 4 layers (300 hPa top), daily, monthly	global, 01/1987-06/1993	Susskind et al., 1997

Table 3: Overview of the G-VAP data archive.

Folder	Parameter	Temporal coverage	Data records
Specific_humidity	Specific humidity at four levels, in g/kg	01/1988 – 12/2009	CFSR, ERA-20C, ERA-Interim, JRA-55, MERRA, MERRA-2, nnHIRS
Temperature	Temperature at four levels, in K	01/1988 – 12/2009	CFSR, ERA-20C, ERA-Interim, JRA-55, MERRA, MERRA-2, nnHIRS
TCWV/long	Total column integrated water vapour, in kg/m^2	01/1988 – 12/2008	CFSR, ERA-20C, ERA-Interim, HOAPS, JRA-55, MERRA, MERRA-2, nnHIRS, Merged Microwave REMSS, NVAP-M, NVAP-O
TCWV/short	Total column integrated water vapour, in kg/m^2	01/2003 – 12/2008	AIRWAVE, AMSR-E JAXA, AMSR-E REMSS, ATOVS, CFSR, EMiR, ERA-20C, ERA-Interim, GOME/SCIAMACHY/GOME-2 GlobVapour, HIRS UWisc, HOAPS, JRA-55, Merged Microwave REMSS, MERIS GlobVapour, MERRA, MERRA-2, MODIS AQUA, nnHIRS, NVAP-M, NVAP-O, SSM/I+MERIS GlobVapour, TMI REMSS

Table A1. Explanation of abbreviations.

AIRS	Atmospheric Infrared Sounder
AIRWAVE	Advanced InfraRed Water Vapour Estimator
(A)ATSR	(Advanced) Along-Track Scanning Radiometer
AVHRR	Advanced Very High Resolution Radiometer
AMSR2	Advanced Microwave Scanning Radiometer 2
AMSR-E	Advanced Microwave Scanning Radiometer for EOS
AMSU-A, -B	Advanced Microwave Sounding Unit-A, -B
(A)TOVS	(Advanced) TIROS Operational Vertical Sounder
ATSR	Along-Track Scanning Radiometer
CFSR	Climate Forecast System Reanalysis
CHAMP	CHAllenging Minisatellite Payload
CM SAF	Satellite Application Facility on Climate Monitoring
COSMIC	Constellation Observing System for Meteorology, Ionosphere, and Climate
CPR	Cloud Profiling Radar
CrIS	Cross-track Infrared Sounder
DMSP	Defense Meteorological Satellite Program
ECMWF	European Centre for Medium-Range Weather Forecasts
ECV	Essential Climate Variables
EMiR	ERS/Envisat MWR Recalibration and Water Vapour TDR Generation
ESA	European Space Agency
EUMETSAT	European Organisation for the Exploitation of Meteorological Satellites
EPS-SG	EUMETSAT Polar System Second Generation
ERA-20C	ECMWF twentieth century reanalysis
ERA-Interim	ECMWF Interim Reanalysis
EUMETSAT	European Organisation for Exploitation of Meteorological Satellites
GCOS	Global Climate Observing System
GDAP	GEWEX Data and Assessments Panel
GEWEX	Global Energy and Water cycle Exchanges
GNSS	Global Navigation Satellite System
GOME, GOME-2	Global Ozone Monitoring Experiment
GPS-RO	Global Positioning System Radio Occultation
GRAS	Global Navigation Satellite System Receiver for Atmospheric Sounding
G-VAP	GEWEX water vapor assessment
HIRS	High Resolution Infrared Sounder
HOAPS	Hamburg Ocean Atmosphere Parameters and Fluxes from Satellite data
HSB	Humidity Sounder for Brazil
IASI	Infrared Atmospheric Sounding Interferometer
ITCZ	Intertropical Convergence Zone
JAXA	Japan Aerospace Exploration Agency
JRA-55	Japanese 55-year Reanalysis
MPI-M	Max Planck Institute for Meteorology
MERIS	Modern Era Retrospective-Analysis for Research and Applications
MERRA, MERRA-2	Modern-Era Retrospective analysis for Research and Applications (Version 2)
Metop	Meteorological Operational Satellite
MHS	Microwave Humidity Sounder
MODIS	Moderate-resolution Imaging Spectroradiometer
MWR	Microwave Radiometer

10.5194/essd-2017-128
Earth System Science Data
2018-01-15

NASA	National Aeronautics and Space Administration
NCEP	National Centers for Environmental Prediction
(N)IR	(Near) InfraRed
NOAA	National Oceanic and Atmospheric Administration
NVAP	NASA Water Vapor Project
NVAP-M	NVAP – Making Earth Science Data Records for Research Environments
OCO-2	Orbiting Carbon Observatory-2
OLCI	Ocean Land Colour Instrument
OMI	Ozone Monitoring Instrument
POLDER	POLarization and Directionality of the Earth's Reflectances
REMSS	Remote Sensing Systems
RMSD	Root Mean Square Difference
ROM SAF	Satellite Application Facility on Radio Occultation Meteorology
SCIAMACHY	Scanning Imaging Absorption Spectrometer for Atmospheric Chartography
SPARC	Stratosphere-troposphere Processes And their Role in Climate
SLSTR	Sea and Land Surface Temperature Radiometer
SSMIS	Special Sensor Microwave Imager
SSM/I	Special Sensor Microwave Imager/Sounder
SSM/T-2	Special Sensor Microwave/Temperature-2
SST	Sea Surface Temperature
T	(profiles of) Temperature
TCWV	Total Column Water Vapour
TES	Technology Experiment Satellite
TIROS	Television Infrared Observation Satellite
TMR	TOPography EXperiment Microwave Radiometer
TMI	Tropical Rainfall Measuring Mission's Microwave Imager
U	University
UCAR	University Corporation for Atmospheric Research
UV	Ultra Violet
vis	visible
WV	(profiles of) Water Vapour
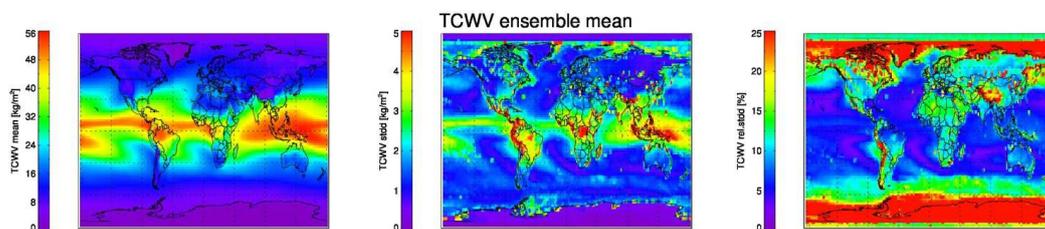
Figure 1: Ensemble mean (left), absolute (middle) and relative (right) standard deviation calculated based on all elements of the G-VAP data archive. Note that the number of available data records differs regionally.
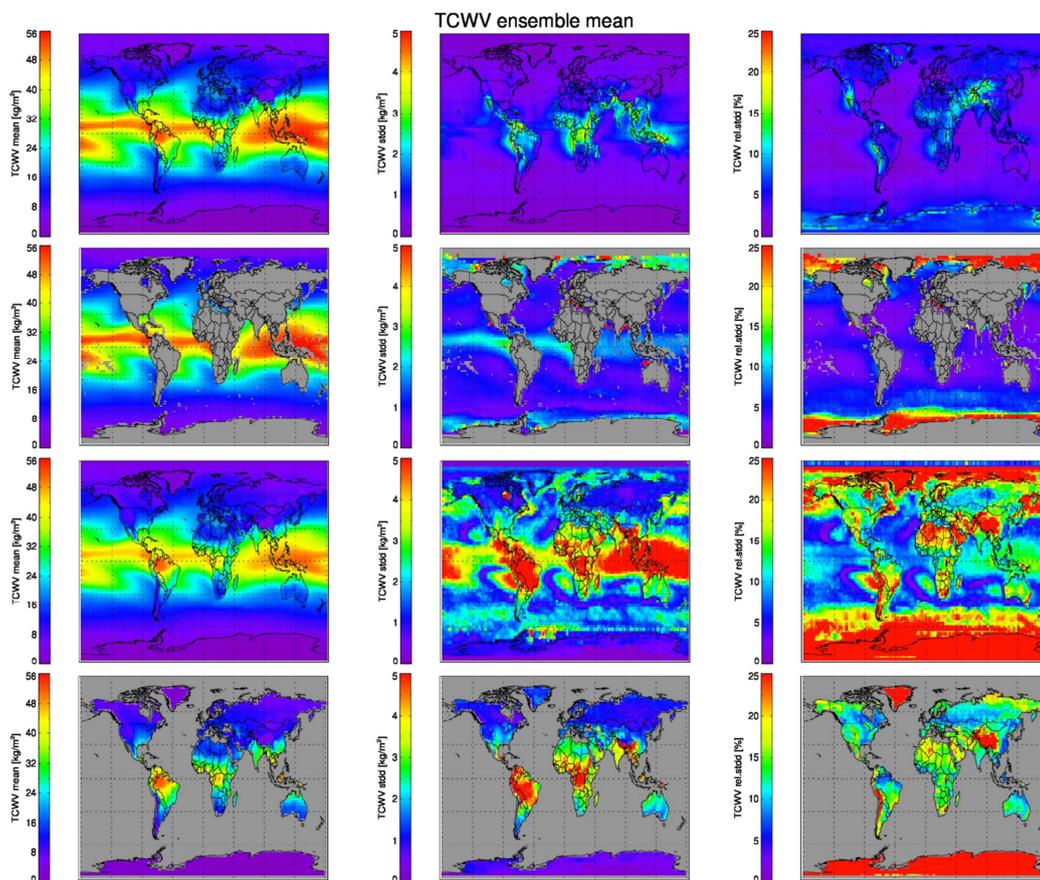
Figure 2: TCWV ensemble means (left), absolute (middle) and relative (right) standard deviations for the different classes of predominant retrieval condition (from top to bottom): all-sky, cloudy-sky, clear-sky (global) and clear-sky over land.
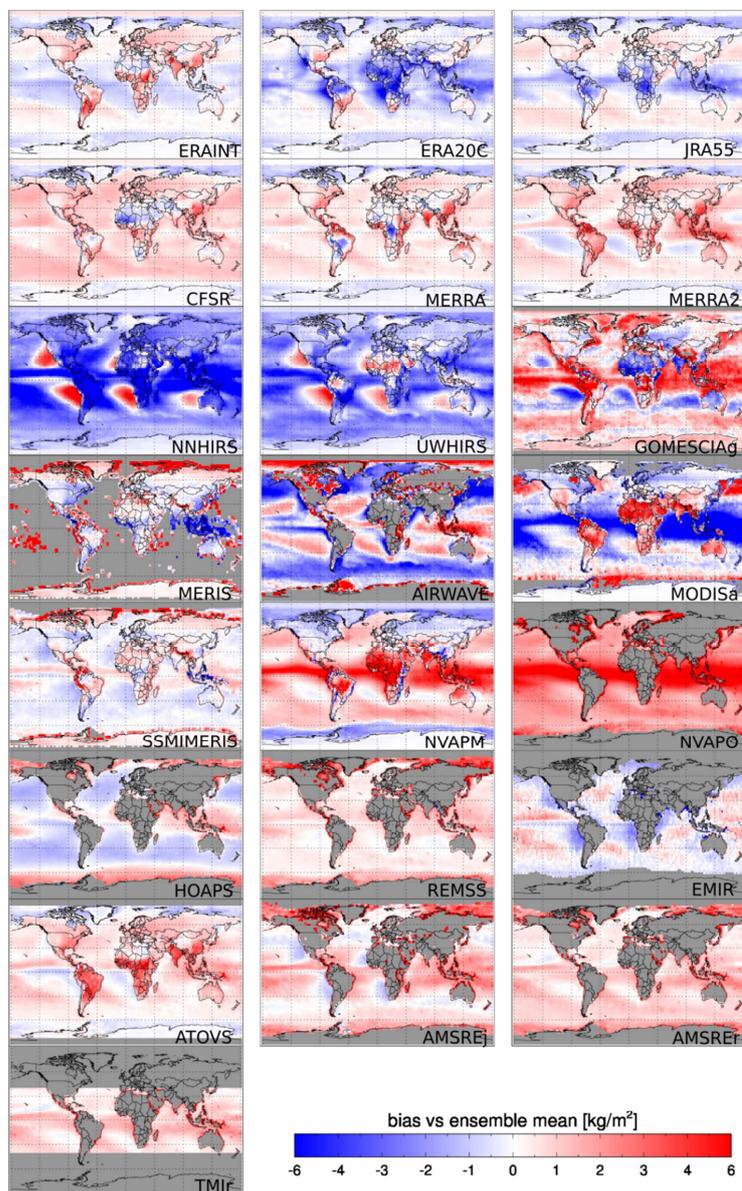
Figure 3: TCWV bias relative to the ensemble mean for all elements of the G-VAP data archive. AQUA, GlobVapour, JAXA and REMSS are abbreviated with "a", "g", "j" and "r".
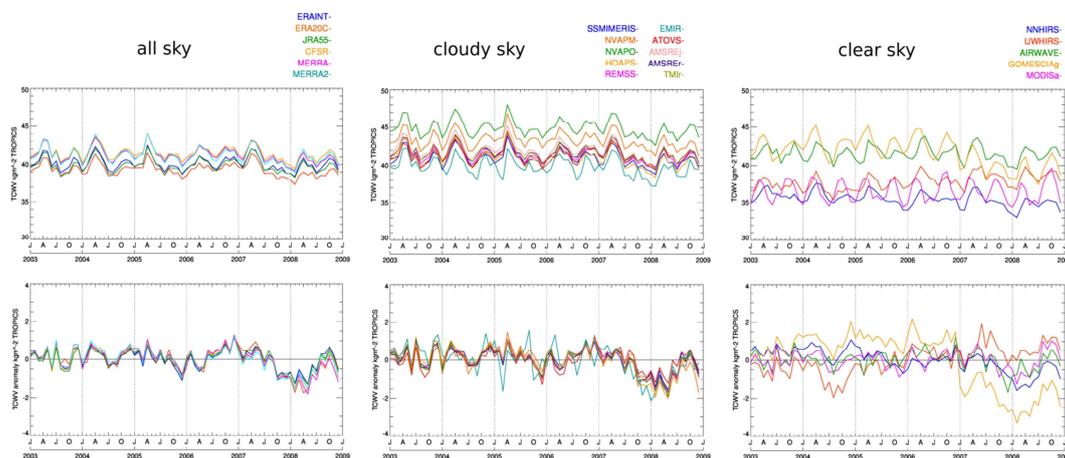
Figure 4: Time series (01/2003 – 12/2008) of TCWV (top) and TCWV anomalies (bottom) for the tropics (±20°N/S) over ocean for the predominant retrieval condition classes all-sky (left), cloudy-sky (middle) and clear-sky (right). MERIS is not shown because it is not defined over ocean. AQUA, GlobVapour, JAXA and REMSS are abbreviated with "a", "g", "j" and "r".